Molecular Pharmacology Fast Forward. Published on December 12, 2008 as doi:10.1124/mol.108.051607
This article has not been copyedited and formatted. The final version may differ from this version.

MOL 51607

Evidence for a direct and functional interaction between the regulators of G protein signaling-2 and phosphorylated C-terminus of cholecystokinin-2 receptor

Ingrid Langer, Irina G. Tikhonova, Cyril Boulègue, Jean-Pierre Estève, Sébastien Vatinel, Audrey Ferrand[2], Luis Moroder[3], Patrick Robberecht[1] and Daniel Fourmy[2]

Université Libre de Bruxelles, Department of Biological Chemistry and Nutrition, Faculty of Medicine, B-1070 Brussels, Belgium (IL, PR).

INSERM, Institut National de la Santé et de la Recherche Médicale, Unit 858, Toulouse, France ; Université de Toulouse 3, Toulouse, France (IGT, JPE, SV, AF, DF)

Max Planck Institut für Biochemie, D-82152 Martinsried, Germany (CB, LM).

Molecular Pharmacology Fast Forward. Published on December 8, 2008 as DOI: 10.1124/mol.108.051607
This article has not been copyedited and formatted. The final version may differ from this version.

MOL 51607

Running title: Basis for recognition of RGS2 by the cholecystokinin-2 receptor

Addresses for correspondence:

Daniel Fourmy, IFR 31, Institut Louis Bugnard, BP 84225, Unité INSERM U858 - I2MR

31432 TOULOUSE CEDEX 4 France, Tel: (33)5 61 32 30 57, Fax: (33)5 61 32 24 03

Email: fourmyd@toulouse.inserm.fr

Number of text pages: 39

Number of tables: 2

Number of figures: 10

Nomber of references: 35

Number of words:

Abstract: 178

Introduction: 723

Discussion: 1488

Non-standard abbreviations used:

CCK, cholecystokinin; RGS2, regulator of G protein signalling-2; HA: hemagglutinin

Molecular Pharmacology Fast Forward. Published on December 8, 2008 as DOI: 10.1124/mol.108.051607
This article has not been copyedited and formatted. The final version may differ from this version.

ABSTRACT

Signaling of G Protein Coupled Receptors (GPCRs) is regulated by different mechanisms, one of these involving regulators of G protein signaling (RGS) which are diverse and multifunctional proteins that bind to active Gα subunits of G proteins and act as GTPase-activating proteins. Little is known about the molecular mechanisms that govern the selective use of RGS proteins in living cells. We first demonstrated that CCK2R-mediated inositol phosphate production, known to be Gq-dependent, is more sensitive to RGS2 than to RGS4 and insensitive to RGS8. Both basal and agonist-stimulated activities of the CCK2R are regulated by RGS2. By combining biochemical, functional and *in silico* structural approaches we demonstrated that a direct and functional interaction occurs between RGS2 and agonist-stimulated cholecystokinin receptor-2 (CCK2R) and identified the precise residues involved: phosphorylated S434 and T439 located in the C-terminal tail of CCK2R and K62, K63 and Q67 located in the N-terminal domain of RGS2. These findings confirm previous reports that RGS proteins can interact with GPCR to modulate their signaling and provide a molecular basis for RGS2 recognition by the CCK2R.

Molecular Pharmacology Fast Forward. Published on December 8, 2008 as DOI: 10.1124/mol.108.051607
This article has not been copyedited and formatted. The final version may differ from this version.

INTRODUCTION

G protein coupled receptors (GPCRs), also referred to as seven transmembrane (TM) domain receptors, represent the largest family of signal transducers for extracellular stimuli. Upon agonist binding, GPCRs undergo conformational changes allowing the interaction of cytoplasmic domains with heterotrimeric G proteins and promoting the exchange of GDP for GTP on the Gα subunit. This initiates the dissociation of the GTP-bound Gα subunit from the Gβγ heterodimer and the activation of downstream effector pathways. Signals are terminated following hydrolysis of Gα-bound GTP and reformation of the inactive trimeric complex (Pierce et al., 2002).

Many mechanisms that operate at the receptor or G protein level have evolved to fine-tune and regulate GPCR signaling. Among these, the most extensively studied is receptor desensitization/internalization which contributes to rapid signaling fading even in the presence of continued agonist exposure. This process involves phosphorylation of receptors in the intracellular loops and/or carboxyl-terminal moiety, binding to β-arrestins followed by binding to clathrin and adaptor protein AP2 (Reiter and Lefkowitz, 2006).

GPCR signaling can also be regulated at post-receptor levels by the regulators of G protein signaling (RGS), a family of diverse and multifunctional proteins that attenuate and/or modulate GPCR-mediated signaling in part by binding to active Gα subunits and by acting as GTPase-activating proteins (GAPs). RGS proteins family members share a conserved 120 amino acid domain, called the RGS box/domain, containing the binding site for Gα and responsible for the GAP activity. They differ in their amino- and carboxy-terminal domains flanking the RGS box that can contain structural domains and binding motifs for a variety of signaling proteins. RGS proteins are classified into six subfamilies based on the RGS box identities and common conserved regions outside the RGS box. The B/R4 subfamily (RGS1, -2, -4, -5, -8, -13 and -16) contains the simplest RGS proteins. Until very recently, they

Molecular Pharmacology Fast Forward. Published on December 8, 2008 as DOI: 10.1124/mol.108.051607
This article has not been copyedited and formatted. The final version may differ from this version.

appeared to have no other function other than modulating G protein activity (Hollinger and Hepler, 2002; Neubig and Siderovski, 2002). In this subfamily, RGS2 and RGS4 are so far the most studied. In particular, the role of exogenous and endogenous RGS2, as a biochemical regulator of levels of inositol trisphosphate and Ca^{2+} oscillation was extensively investigated in permeabilized pancreatic acini from rat and from $RGS2^{-/-}$ mice, respectively (Luo et al., 2001; Wang et al., 2004). The *in vivo* function of RGS2 as an essential signaling molecule was shown in $RGS2^{-/-}$ mice presenting several abnormalities including hypertension, prolonged vasoconstrictor signaling and anxiety (Heximer et al., 2003; Oliveira-Dos-Santos et al., 2000).

The biochemical mechanisms of GAP activity and the structure of RGS proteins have been well characterized, however, little is known about the cellular mechanisms that regulate RGS proteins recruitment and use, although, RGS proteins appear to regulate Gα functions through recognition of receptor in addition to their association with Gα (Wang et al., 2002; Zeng et al., 1998). Early evidence for RGS recognition by GPCR came from Xu and co-workers who reported that in pancreatic acinar cells, RGS1, -2, -4 and -16 displayed different regulatory potency toward Gq/11-dependent Ca^{2+} signaling in response to activation of three different GPCRs, the muscarinic cholinergic, bombesin or cholecystokinin receptors (Xu et al., 1999). Since this early finding, a molecular mechanism for regulation of muscarinic receptor M1 by RGS2 involving a direct interaction was reported (Bernstein et al., 2004, and discussion) but the precise explanation that different RGS display different potencies towards Gq/11-dependent Ca^{2+} signaling in response to activation of distinct receptors remains unknown.

Given our specific interest towards the cholecystokinin-2 receptor, we wanted to investigate the mechanism whereby signaling of this receptor is regulated by RGS proteins. The Cholecystokinin (CCK)-2 receptor (CCK2R), belongs to family A of rhodopsin-like

Molecular Pharmacology Fast Forward. Published on December 8, 2008 as DOI: 10.1124/mol.108.051607
This article has not been copyedited and formatted. The final version may differ from this version.

GPCRs. It binds both cholecystokinin and gastrin, with a similar, high affinity (Dufresne et al., 2006). The CCK2R is expressed in the central nervous system and in the gut where it represents the predominant CCK receptor subtype (Dufresne et al., 2006; Noble et al., 1999). CCK2R mediates a wide spectrum of CCK- and gastrin-induced biological effects including anxiety, pain perception and gastric acid secretion, as well as controlling growth and differentiation of the gastric mucosa.

In the work presented here, we provided experimental evidences that a direct high affinity and functional interaction occurs between the human CCK2R and RGS2 and identified the interacting residues in the C-terminal phosphorylated region of CCK2R and in the N-terminal moiety of RGS2.

Molecular Pharmacology Fast Forward. Published on December 8, 2008 as DOI: 10.1124/mol.108.051607
This article has not been copyedited and formatted. The final version may differ from this version.

MATERIALS AND METHODS

Materials. Sulfated [Thr^{28},Nle^{31}]-CCK25-33 (CCK9s) was synthesized as described (Moroder et al., 1981). [^{125}I]-Na (2000 Ci/mmole) was from Amersham Biosciences (Les Ulis, France). Sulfated [Thr^{28},Nle^{31}]-CCK25-33 was conjugated with Bolton-Hunter reagent, purified and radioiodinated as described previously and is referred as [^{125}I]-CCK9s (Fourmy et al., 1989).

Site-directed mutagenesis and transfection of COS-7 cells. All mutant receptor cDNAs were constructed by oligonucleotide-directed mutagenesis (Quick-Change^{TM} site-directed mutagenesis kit, Stratagene, France) using the human CCK2R cDNAs with HA or MYC epitope TAG at the amino-terminus cloned into pRFENeo vector as template. Truncated receptors at the C-terminus were obtained by introducing a stop codon (TGA) at position 410 (CCK2[1-409]), 430 (CCK2[1-429]) or 440 (CCK2[1-439]). The cDNA for mouse RGS2 with an HA epitope TAG at the amino-terminus subcloned into pCR3.1 was a gift from Luc De Vries. The cDNA for human RGS4 and RGS8 with HA epitope TAG at the amino-terminus subcloned into pcDNA3.1 was obtained from the UMR cDNA Resource Center (www.cdna.org). Truncated RGS2 at the N-terminus were obtained by insertion of a BamHI restriction site followed by an initiating methionine at position 24-26 (RGS2[28-211]), 51-53 (RGS2[54-211]) or 77-79 (RGS2[80-211]) by using oligonucleotide-directed mutagenesis. Modified plasmids were then digested by BamHI and XhoI restriction enzymes to allow excision of RGS2 sequences [28-211], [54-211] or [80-211] that were then subcloned into pCR3.1 vector. For these truncated RGS2 constructs an HA epitope TAG was then inserted at the C-terminus by site directed mutagenesis. The presence of the desired and the absence of undesired mutations were confirmed by automated sequencing of the complete sequence (Applied Biosystem).

Molecular Pharmacology Fast Forward. Published on December 8, 2008 as DOI: 10.1124/mol.108.051607
This article has not been copyedited and formatted. The final version may differ from this version.

Transfection of COS-7 cells. COS-7 cells (1.5 x 10^6) were plated onto 10 cm culture dishes and grown in Dulbelcco's Modified Eagle's Medium (DMEM) containing 5% fetal calf serum in a 5% CO_2 atmosphere at 37 °C. After overnight incubation, cells were transfected with 0.5 μg/plate of pRFENeo vectors containing the cDNA for the wild-type or mutated CCK_2 receptors in absence or in presence of vectors containing the cDNA for the wild-type or mutated RGS, using a modified DEAE-dextran method as described previously (32). In each experiment the total amount of DNA/plate was adjusted to 2.5 μg with empty pCR3.1 or pcDNA3.1 plasmids. Cells were transferred to 24 well plates at a density of 20,000 (binding studies) or 150,000 (Ins-P assay) cells/well 24 h after transfection.

Receptor binding assay. Approximately 24 h after the transfer of transfected cells to 24 well plates, the cells were washed with phosphate-buffered saline (PBS) pH 7.4 containing 0.1% BSA (Bovine Serum Albumin) and then incubated for 60 min. at 37°C in 0.3 ml DMEM containing 0.1% BSA with 50 pM [^{125}I]-CCK9s in the presence or in the absence of unlabelled CCK9s. The cells were washed twice with cold PBS pH 7.4 containing 2% BSA and cell associated radioligand was collected by cell lysis with NaOH 0.1N. The radioactivity was directly counted in a gamma counter (Auto-Gamma, Packard, Downers Grove, IL). Receptor density (Bmax) and dissociation constant (Kd) were calculated from homologous [^{125}I]-CCK9s/CCK9s competition binding experiments using Ligand software (Kell, Cambridge, UK).

Inositol phosphates assay. Approximately 24 h after the transfer to 24-wells plates and following overnight incubation in DMEM containing 2 μCi/ml of myo-2-[3H]inositol, (Amersham biosciences, Les Ulis, France), the transfected cells were washed with DMEM and then incubated for 30 min. in 1 ml/well DMEM containing 20 mM LiCl at 37°C. The cells were washed with IP buffer at pH 7.45 : PBS containing 135 mM NaCl, 20 mM HEPES, 2 mM $CaCl_2$, 1.2 mM $MgSO_4$, 1 mM EGTA,10 mM LiCl, 11.1 mM glucose and

Molecular Pharmacology Fast Forward. Published on December 8, 2008 as DOI: 10.1124/mol.108.051607
This article has not been copyedited and formatted. The final version may differ from this version.

0.5% BSA. The cells were then incubated for 60 min. at 37°C in 0.3 ml IP buffer with or without increasing CCK9s concentration. The reaction was stopped by adding 1 ml methanol/HCl to each well and the content was transferred to a column (Dowex AG 1-X8, formate form, BioRad, Hercules, CA) for the determination of inositol phosphate. The columns were washed twice with 3 ml distilled water and twice with 2 ml of 5 mM sodium tetraborate/60 mM sodium formate. The content of each column was eluted by addition of 2 ml of 1 M ammonium formate/100 mM formic acid. Radioactivity of 1 ml of the eluted fraction was evaluated using a liquid scintillation counter (Packard Instrument Co). EC_{50} (potency) which corresponded to concentrations of CCK9s giving half-maximal stimulation were calculated from dose-effect curves by non linear regression curve fitting using GraphPad Prism software (San Diego, USA). Maximal efficacy (Emax) corresponded to inositol phosphate production achieved in the presence of supramaximal concentrations of CCK.

Preparation of COS-7 cells lysate. 36 to 48h after transfection, cells were washed twice with PBS and once with buffer consisting in 50 mM Hepes, 150 mM NaCl, 10 mM EDTA, 10 mM $Na_4P_2O_7$, 100 mM NaF, 2 mM orthovanadate pH 7.5. Cells were then lysed following 30 min. incubation on ice in the same buffer containing 1.5% CHAPS and protease inhibitors cocktail (Complete®, Roche). The remaining insoluble material was eliminated by centrifugation at 15.000 g for 10 min. at 4°C. Protein concentration was evaluated by using BCA assay kit (Pierce et al.).

Western Blot. Protein samples were subjected to 12% SDS-polyacrylamide gel electrophoresis and then electroblotted to nitrocellulose membrane. Nitrocellulose membrane was incubated in blocking buffer (PBS + 3% milk + 0.1% tween 20) for 1 hour at room temperature then probed with mouse anti-HA antibody (Covance) diluted 1:1000 in PBS + 1% milk + 0.1% tween 20 overnight at 4°C. Membranes were washed three times in PBS +

Molecular Pharmacology Fast Forward. Published on December 8, 2008 as DOI: 10.1124/mol.108.051607
This article has not been copyedited and formatted. The final version may differ from this version.

0.1% tween 20, then probed with HRP goat anti-mouse antibody (Pierce et al.) diluted 1:50.000 in PBS + 0.1% tween 20 for 1 hour at room temperature. Proteins were visualized using SuperSignal® West Pico Chemiluminescent Substrate (Pierce et al.). To verify that the same amount of protein was loaded on the gel, the membranes were stripped and re-probed using a mouse anti-GAPDH antibody (Chemicon) diluted 1:5000 as described here upper.

Pull down assay. Lysates of COS-7 cells expressing wild type or mutated HA-CCK2R were mixed with 100 µg biotinylated fragment of RGS2 (sequence 54-79) bound to 250 µl sepharose-streptavidine beads (GE Healthcare) and incubated by rotating overnight at 4°C. Beads were pelleted, washed 10 times with buffer containing 20 mM NaH_2PO_4 and 150 mM NaCl pH 7.5, bound proteins were eluted with SDS sample buffer. Samples were boiled for 5 min, centrifuged briefly to pellet beads, resolved on 9% SDS-PAGE and transferred to nitrocellulose membrane. Membrane was probed with mouse anti-HA antibody (Covance) diluted 1:1000 as described upper.

Immunoprecipitation and determination of receptor phosphorylation levels. 32 hours after transfection with HA-CCK2R constructs, COS-7 cells were cultured in phosphate-free DMEM medium for 16 hours and then incubated for 2 hours at 37°C in same medium containing 200 µCi acid-free [^{32}P]-orthophosphate (MP Biomedicals). At the end of this labelling period, CCK9s was added. After agonist exposure, cells were washed three times with ice-cold buffer consisting in 10 mM HEPES, 4.2 mM $NaHCO_3$, 11.7 mM glucose, 1.2 mM $MgSO_4$, 4.7 mM KCl, 118 mM NaCl and 1.3 mM $CaCl_2$ pH 7.4 and then lysed as described here upper. The cell lysate was added to 30 µl of a protein G sepharose suspension (GE Healthcare) previously coated during 30 min. with 1 µl of mouse anti-HA antibody (Covance). After overnight incubation under light agitation at 4°C, the sepharose beads were separated by centrifugation and washed five times with buffer consisting in HEPES 30 mM, NaCl 30 mM and Triton X-100 1% pH 7.5. The final beads pellet was resuspended in SDS

Molecular Pharmacology Fast Forward. Published on December 8, 2008 as DOI: 10.1124/mol.108.051607
This article has not been copyedited and formatted. The final version may differ from this version.

sample buffer. After heating at 95°C for 5 min., the samples were resolved by SDS page using 9% gel. The gel was fixed, dried and the phosphorylated bands detected and quantified by phosphoimaging.

Purification of recombinant RGS2 proteins. RGS2 and RGS2[80-211] DNA sequences inserted into pCR3.1 vector were digested by BamHI and XhoI restriction enzymes and then subcloned into pET28a vector (Novagen) for bacterial expression with a N-terminal hexa-histidine tag. RGS2 and RGS2[80-211] in pET28a were transformed into BL21(DE3) *E. Coli*. For each protein, one liter culture was grown in LB/kanamycin and induced with 1 mM isopropyl-β-D-thiogalactopyranoside for 2h at 37°C. Bacteria were kept 5 min. on ice then pelleted. The pellets were frozen at -80°C overnight and then resuspended in 25 ml of binding buffer (Na_2HPO4 20 mM, NaCl 0.5 M, 20 mM imidazole, triton 1% pH 7.4) supplemented with Complete® protease inhibitor cocktail (Roche) and snap-frozen two times in liquid nitrogen. Bacteria were thaw, sonicated, kept on ice 30 min. followed by centrifugation at 15.000g at 4°C for 20 min. to collect soluble materials. The supernatant was then incubated with 1.5 ml Nickel equilibrated Chelating Sepharose Fast Flow (GE Healthcare) for 2 hours at 4°C. After incubation, sepharose beads were pelleted, washed 3 times with 7,5 ml wash buffer (Na_2HPO4 20 mM, NaCl 0.5 M, 100 mM imidazole, triton 1% pH 7.4) and eluted with elution buffer (Na_2HPO4 20 mM, NaCl 0.5 M, 200 mM imidazole pH 7.4). Proteins were then purified and concentrated by ultrafiltration using a 10 kDa cut-off membrane (Centricon, Millipore). Protein concentration was determined by Bradford reagent (Bio-Rad) and was estimated to be 90% pure as determined by coomassie blue staining of SDS-PAGE gel.

Purification of the CCK2 receptor third intracellular loop. The sequence corresponding to the third intracellular loop of the human CCK2 receptor (3il[244-335]) was subcloned into the bacterial expression vector pGEX-4T2 (GE Healthcare) with a N-terminal GST tag. E. coli

Molecular Pharmacology Fast Forward. Published on December 8, 2008 as DOI: 10.1124/mol.108.051607
This article has not been copyedited and formatted. The final version may differ from this version.

BL21 strains were then transformed with this construct and grown in 500mL LB/Ampicillin medium. Protein production was induced by IPTG addition (1mM) for 90 min. at 30°C. After centrifugation bacteria pellets were resuspended in a lysis buffer (10mM Tris, 60mM NaCl, 1mM EDTA, 1% Triton X100, protease inhibitors), snap-frozen two times in liquid nitrogen and sonicated. Lysates were then kept for 30 min. at 37°C with 50UI/mL DNase I, 2mM DTT, 2.5mM $MgCl_2$ and centrifugated at 12000 rpm for 30min. Supernatants were collected and incubated overnight with glutathione beads (Sigma Aldrich). The GST-3il[244-335] protein was eluted with 10mM glutathione-reduced. Proteins were purified and concentrated by ultrafiltration using 10kDa cut-off membrane and their concentration determined by Bradford reagent (Bio-Rad). GST-3il[244-335] was estimated to be pure over 90% by coomassie blue staining of SDS-PAGE gel.

Surface plasmon resonance analysis. Surface plasmon resonance experiments were carried out on a BIA-core 3000 instrument (BIAcore AB). The biotinylated peptides corresponding to C-terminal moiety of CCK2R: CCK2R[429-445], Biot-GGG-SIASLSRLSYTTISTLG; pS434T439, Biot-GGG-SIASLS*(PO3)*RLSYTTISTLG and pS434pT439, Biot-GGG-SIASLS*(PO3)*RLSYT*(PO3)*TISTLG were synthesized on an Applied Biosystems model Pioneer™ Peptide Synthesis System using the standard procedures of Fmoc/tBu chemistry on a Tentagel S Ram resin from Rapp polymer. Biotinylation was performed manually and peptides were obtained after a 2 h treatment with trifluoroacetic acid (TFA)/Water/Triisopropylsilane (TIPS) (95/2.5/2.5) or Reagent B (TFA/Phenol/H_2O/TIPS 88/5/2,5/2,5) followed by precipitation in cold Methyltert-butylether/hexane (2/1). All peptides were purified to high homogeneity (≥95%) by RP-HPLC and their molecular weights verified by electrospray ESI-MS.

The biotinylated peptides were immobilized on chips with streptavidin coated matrix (Chip SA BIAcore). GST-3il[244-335] was immobilized on corboxymethylated dextran

Molecular Pharmacology Fast Forward. Published on December 8, 2008 as DOI: 10.1124/mol.108.051607
This article has not been copyedited and formatted. The final version may differ from this version.

matrix (chip CM5 BIAcore) via standard EDC/NHS amine coupling (BIAcore). Different concentrations of hexahistidine-RGS2 and hexahistidine-RGS2[80-211] were passed over the immobilized peptides or GST-3il[244-335] protein and, kinetic and affinity constants were determined using BIAevaluation 4.0 software (BIAcore).

Molecular Modeling. The 3D-model of RGS2 in water-lipid environment described previously (Tikhonova et al., 2006) was used for the investigation of RGS2 interactions with the C-terminal part of CCK2R (429-447 residues). The fully flexible docking of the C-terminal part of CCK2R in unphosphorylated/phosphorylated forms to RGS2 was done using Gold program (Jones et al., 1997). Each docking pose of the C-terminal part of CCK2R was evaluated by fitness scoring implemented in Gold and also visual inspection. The final complex of the C-terminal part of CCK2R and RGS2 was chosen based on the experimental validations. To investigate the stability of the interactions between RGS2 and the C-terminal part of CCK2R obtained from the docking studies, the final complex was submitted to 1 ns molecular dynamics simulation in water-lipid environment using Gromacs program (Van Der Spoel et al., 2005). For this purpose, we have used the coordinates of RGS2 and lipids that we obtained previously (Tikhonova et al., 2006) where the C-terminal part was implemented and the whole system was solvated and neutralized. The system was then minimized and submitted to molecular dynamics simulation. The protocol for the simulation was the same as described (Tikhonova et al., 2006). In brief, the simulation was performed at 310K, the time step for integration was 2fs, and LINCS algorithm was used to restrain bond lengths.

Molecular Pharmacology Fast Forward. Published on December 8, 2008 as DOI: 10.1124/mol.108.051607
This article has not been copyedited and formatted. The final version may differ from this version.

RESULTS

RGS2 modulates CCK2R-mediated inositol phosphate production.

CCK2R is a G-coupled receptor widely expressed in peripheral tissues and in the central nervous system. CCK2R-mediated biological effects result from a signaling cascade starting with Gq-dependent activation of phospholipase C (Dufresne et al., 2006; Marco et al., 2007). In order to identify potential RGS proteins involved in the modulation of CCK2R-mediated signaling, we expressed in COS-7 cells CCK2R in the absence, or presence of increasing amounts of RGS2, RGS4 (both recognized regulators of Gq), or RGS8 (a regulator of Gi/o and Gq). As shown in Fig. 1, basal (Fig. 1A) and CCK-induced (1 μM) (Fig. 1B) inositol phosphate accumulation decreased in cells expressing RGS2 or RGS4 but not in those expressing RGS8. RGS2 effects were concentration-dependent as shown by titration experiments with increasing amounts of transfected RGS coding plasmids (Fig. 1C). In all conditions, CCK potency and affinity were unaffected (data not shown). We next examined, whether changes in the expression level of CCK2R could be at the origin of reduced signaling in the presence of increasing concentrations of RGS2 or RGS4. Regardless of the amount of RGS plasmid used, CCK2R expression levels were not significantly affected by co-expression of RGS2 or RGS8 but were slightly reduced in RGS4 expressing cells (See Fig. 1 legend). The reason for the slight decrease of CCK2R expression in RGS4 expressing cells is unknown. However, this first series of data clearly supports that RGS2 is the most efficient regulator of both basal and CCK-stimulated CCK2R-mediated inositol phosphate production.

An internal sequence within the N-terminal domain of RGS2 is required for RGS2 regulation of CCK2R-mediated inositol phosphate production.

RGS2 is composed of an N-terminal region (RGS2[1-80] comprising an amphipathic helix), a central RGS box (RGS2[80-200] responsible for Gα subunit binding and GAP activity) and a short C-terminal domain (RGS2[201-211]) (Kehrl and Sinnarajah, 2002). In

Molecular Pharmacology Fast Forward. Published on December 8, 2008 as DOI: 10.1124/mol.108.051607
This article has not been copyedited and formatted. The final version may differ from this version.

order to determine if another region than the RGS box could be involved in the inhibitory effects of RGS2 on CCK2R-mediated inositol phosphate production, we evaluated the activity of truncated forms of RGS2 missing the first 27 (RGS2[28-211]), 53 (RGS2[54-211]) or 79 (RGS2[80-211]) N-terminal amino acids (Fig. 2A). Since wild-type CCK2R was previously demonstrated to exhibit a constitutive activity leading to production of inositol phosphates in absence of agonist stimulation (Foucaud et al., 2006; Marco et al., 2007), effects of RGS2 and truncated variants were tested both on basal and CCK-stimulated production of inositol phosphates in cells. As shown in Fig. 2, RGS2[1-211], [28-211] and [54-211] were equally active on both basal (Fig. 2B) and CCK-induced (1 μM) (Fig. 2C) inositol phosphate accumulation, whereas deletion of the entire N-terminal domain of RGS2 (RGS2[80-211]) completely abolished the RGS2 inhibitory effect. As with full-length RGS2, the inhibitory effect of active truncated RGS2 was concentration-dependent (Fig. 2D) and the exogenous co-expression of truncated RGS2 did not modify CCK potency and affinity or CCK2R expression levels (See Fig. 2 legend). These results thus support that the RGS2 sequence [54-79] is required for RGS2 inhibition of CCK2R-mediated inositol phosphate production. This sequence [54-79] has not yet been reported as critical for RGS2 activity. Of interest, it comprises neither the amphipathic helix likely involved in RGS proteins recruitment to membrane, nor the RGS box which comprises Gα subunit binding domain and GAP activity domain (Kehrl and Sinnarajah, 2002).

We further tested the hypothesis that sequence [54-79] of RGS2 may be physically involved in a functional complex including CCK2R. We carried out pull-down experiments using immobilized amino-biotinylated peptide corresponding to sequence 54 to 79 of RGS2 and solubilized from COS-7 cells expressing HA-CCK2R. We found that immobilized RGS2[54-79] fragment adsorbed a 80 kDa-protein specifically revealed by an anti-HA

Molecular Pharmacology Fast Forward. Published on December 8, 2008 as DOI: 10.1124/mol.108.051607
This article has not been copyedited and formatted. The final version may differ from this version.

antibody (Fig. 3). No specific protein band was observed after immobilization of irrelevant biotinylated peptide.

To evaluate whether the sequences identified are indeed involved in RGS2.CCK2R complex formation in a cellular context, we co-expressed HA-RGS2 constructs and MYC-CCK2R constructs in COS-7 cells and studied their cellular localization by immunofluorescence. When expressed alone in COS-7 cells HA-RGS2, HA-RGS2[28-211], HA-RGS2[54-211] and HA-RGS2[80-211] localized in the cytoplasm and in the nucleus and (supplementary data). After co-transfection with MYC-CCK2R, HA-RGS2 and HA-RGS2[28-211] primarily co-localized with the MYC-CCK2R at plasma membrane, HA-RGS2[54-211] co-localized in part with MYC-CCK2R at the plasma membrane while RGS2[80-211] remained in intracellular compartments (supplementary data).

All together, *in cellulo* studies with truncated RGS2 and pull-down experiments suggest that sequence [54-79] located in the N-terminus of RGS2 is critical for the ability of RGS2 to modulate CCK2R mediated signaling and is potentially involved in a signaling complex including CCK2R.

A sequence in the C-terminal tail of CCK2R is required for RGS2 regulation of CCK2R-mediated inositol phosphate production.

We next attempted to identify regions in CCK2R which are critical for RGS2 regulation of CCK2R mediated signaling. We first considered the C-terminal tail of CCK2R as a candidate sequence due to frequent involvement of this region in GPCRs in multiple regulatory processes. Co-expression of RGS2 and CCK2R truncated in position 409 (CCK2[1-409]) or 429 (CCK2[1-429]) did not affect CCK-induced inositol phosphate production by the receptor mutants. However, the RGS2 inhibitory effect was partially restored for the CCK2[1-439] mutant suggesting that a sequence between residues 429 and

Molecular Pharmacology Fast Forward. Published on December 8, 2008 as DOI: 10.1124/mol.108.051607
This article has not been copyedited and formatted. The final version may differ from this version.

439 was required for RGS2 inhibitory effect on inositol phosphate production (Fig. 4, table I). In contrast, the RGS2 inhibitory effect on basal inositol phosphate production was preserved for all truncated receptors tested (Table I). We did not observe any changes in CCK affinity or receptor density (Table I). Despite similar receptor densities, maximal inositol phosphate responses with truncated receptors were enhanced by about 2 fold compared to the wild-type CCK2R response. Basal inositol phosphate production was also enhanced by 1.5 fold with CCK2[1-409]. (Fig. 5, Table I). In order to determine whether the effect on truncated CCK2R seen in the absence of RGS2 was caused by the loss of interaction between RGS2 and CCK2R, we carried out pull-down experiments. As shown in Fig. 5, CCK2[1-439] but not CCK2[1-409] was adsorbed on the RGS2 fragment.

All together, these results suggest that inhibitory action of RGS2 on CCK2R-mediated production of inositol phosphates following agonist stimulation occurs through formation of a functional complex comprising RGS2 and CCK2R and involving the sequence [54-79] in RGS2 and a sequence down-stream amino acid 429 in the CCK2R.

Evidence that phosphorylated Ser434 and Thr439 located in the C-terminus of CCK2R are critical for RGS2 ability to modulate CCK2R-mediated inositol phosphate production.

We first examined the theoretical possibility of direct interaction between RGS2 and CCK2R by docking the C-terminal peptide (429-447 residues) of CCK2R to modeled RGS2. In our previous report (Tikhonova et al., 2006), we built the three-dimensional (3D) model of the RGS2, including its N-terminal moiety, in several steps. Since the crystal of the RGS2 box was not available at the time of construction, we employed the crystal of the RGS4 box interacting with Gαi1 protein (http://www.rcsb.org/, PDB code: 1AGR) to build the RGS2 box (Tikhonova et al., 2006) using homology modeling. Superimposition of our homology

Molecular Pharmacology Fast Forward. Published on December 8, 2008 as DOI: 10.1124/mol.108.051607
This article has not been copyedited and formatted. The final version may differ from this version.

model of RGS2 with coordinates of RGS2 crystal subsequently released (http://www.rcsb.org/, PDB code: 2AF0) gives high degree of concordance. We then constructed separately the N-terminal region of RGS2 using the protein structure prediction server ROBETTA (http://www.robetta.net/) and data from circular dichroism spectroscopy analysis of RGS2 N-terminal fragment (39-79 residues) solubilized from COS-7 cells expressing HA-CCK2R (Tikhonova et al., 2006). Lastly, we assembled the N-terminal part of RGS2 to our model of the RGS2 box and optimized in water-lipid environment during 5 ns to assess protein stability (details in (Tikhonova et al., 2006)). In the current work, to examine theoretical possibilities of a direct interaction between RGS2 and CCK2R, we attempted to dock the C-terminal peptide (429-447 residues) of CCK2R to this 3D-model of RGS2. Although, during the docking, the C-terminal peptide was fully flexible, we could not find any plausible contacts between two proteins. We then considered that the C-terminal peptide of CCK2R containing a number of Ser and Thr residues represented potential sites of phosphorylation. These could be theoretically predicted using the NetPhos server (Blom et al., 1999). We therefore carried out a second docking experiment considering the C-terminal part phosphorylated either on S432, S434, S437, Y438 or T439. All obtained complexes showed energetically favorable contacts with positively charged residues K57, K62 and K63 of RGS2 (not shown).

To evaluate the potential contribution of S432, S434, S437, Y438 and T439 located in the C-terminus of CCK2R to the inhibitory effect of RGS2, we exchanged Ser/Thr residues for Ala and Y438 for Phe. For all mutants tested, the inhibitory effect of RGS2 on basal inositol phosphate production was preserved. In contrast, mutation of S434 or T439 to Ala reduced (S434A) or fully abolished (T439A, S434AT439A) the ability of RGS2 to modulate CCK-induced inositol phosphate accumulation (Fig. 6 and Table II). CCK potency and affinity were similar to that observed for the wild type receptor either in the absence or the

Molecular Pharmacology Fast Forward. Published on December 8, 2008 as DOI: 10.1124/mol.108.051607
This article has not been copyedited and formatted. The final version may differ from this version.

presence of RGS2. Receptor binding assay indicated that all cell preparations expressed a similar receptor density (Table II). We next evaluated the effect of mutations of S434 or T439 to glutamate, a residue known to mimic phosphorylated Ser/Thr residues. As shown in Table II, the effect of RGS2 was restored in cells expressing S434E mutant but not T439E mutant.

Although well established for other GPCR, phosphorylation of CCK2R by GRK following repeated or sustained exposure to agonists has not yet been documented. We therefore investigated if S434 and T439 were indeed phosphorylated following CCK exposure in living cells. As shown in Fig. 7A, CCK induced a rapid, dose-dependent stimulation of [^{32}P] incorporation into a protein with an apparent molecular size of 85 kDa that was immunoprecipitated with the anti-HA antibody. The maximal signal was obtained following 5 min stimulation with 100 nM CCK. As shown in Fig. 7B, mutation of S434 and T439 to alanine (a non-phosphorylatable residue) led to 36 ± 8% reduction in CCK2R phosphorylation after normalization of the signal with receptor expression levels.

We further used plasmon resonance technology to experimentally verify *in vitro* whether a direct interaction between RGS2 and a phosphorylated C-terminal moiety of CCK2R can occur in the absence of any other cell proteins. We tested the binding to recombinant RGS2 of synthetic replicates of the C-terminal tail of CCK2R which were biotinylated on the N-terminus and either phosphorylated or not on both S434 and T439, or phosphorylated only on S434. We observed a clear interaction between the immobilized CCK2R fragment doubly phosphorylated on S434 and T439 (pS434pT439) and RGS2, but no specific binding for the mono-phosphorylated CCK2R fragment (pS434T439) or the non-phosphorylated C-terminal of CCK2R used as a reference peptide to overcome nonspecific interactions between RGS2 and dextran carboxymethylated chips (Fig. 8A). Binding of RGS2 was dose-dependent (500 nM - 8 μM) (Fig. 8B) and was completely abolished after removal of the N-terminal region of RGS2 (data not shown). Global fitting of these interactions

Molecular Pharmacology Fast Forward. Published on December 8, 2008 as DOI: 10.1124/mol.108.051607
This article has not been copyedited and formatted. The final version may differ from this version.

resulted in an affinity constant of 79 ± 2 nM (calculated as the ratio between K_{off} and K_{on}) and a maximal binding of 600 ± 50 resonance units. We also tested the hypothesis that a direct interaction between the third intracellular loop of the CCK2R and RGS2 may occur. However, plasmon resonance experiments could not detect any specific binding between recombinant RGS2 and a GST-fusion protein corresponding to the third intracellular loop of the CCK2R (GST-3il[244-335]) (data not shown).

All together, these *in silico* and laboratory data strongly support the idea that regulation of CCK2R-mediated inositol phosphate production by RGS2 involves a direct interaction between the C-terminal phosphorylated of the human CCK2R and an internal sequence in the N-terminal region of RGS2.

Identification of amino acids within the N-terminal region of RGS2 which participate to CCK2R recognition.

Starting with all available experimental results from the current study, the 3D model of the complex between RGS2 and C-terminal tail of CCK2R phosphorylated on S434 and T439 was chosen and optimized in a water-lipid environment. During simulation, stable contacts were achieved including ionic interactions involving phospho-S434 (pS434 in CCK2R) and K62 (RGS2), phospho-T439 (pT439 in CCK2R) and K63 (RGS2) as well as a hydrogen bond between pT439 and Q67 (RGS2) (Fig. 9). To further assess the molecular basis for specific recognition of RGS2, we first considered sequence alignment of the three RGS proteins tested in the current study. Alignment indicated that in spite of some homology, the N-terminal sequence of RGS8 differs from that of RGS2, especially at positions crucial for interaction. In contrast, RGS4 and RGS2 present strong homology in the loop of interest, except Q67 which in the modeled complex (Fig. 9) interacts with pT439 and is not present in RGS4. On this basis, we hypothesized that Q67 may represent a key amino acid for specific recognition of CCK2R. We evaluated the effect of a mutation of Q67 to Ala and found that the RGS2-Q67A

Molecular Pharmacology Fast Forward. Published on December 8, 2008 as DOI: 10.1124/mol.108.051607
This article has not been copyedited and formatted. The final version may differ from this version.

mutant displayed 50% reduced efficacy in inhibiting CCK-induced inositol phosphate accumulation as compared to *bona fide* RGS2 (data not shown). We then replaced the 59-67 sequence of RGS2 by the corresponding sequence of RGS4 (residues 36 to 45) and replaced the 36-45 sequence of RGS4 by the corresponding sequence of RGS2 (residues 59 to 64) and examined loss or gain of function of the chimeric RGS2/RGS4. The choice of the sequences replaced in chimeric RGS protein constructs was driven by: 1) amino acids (K62, K63 and Q67) identified by molecular modeling as interacting partners of phosphorylated S434 and T439 of CCK2R, 2) the presence of a proline (P59) upstream of K62, K63 and Q67 in RGS2 that is not conserved in RGS4 and that may account for correct positioning and access of these amino acids. As shown in Fig. 10, the replacement of the PKTGKKSKQQ sequence in RGS2 by the corresponding sequence in RGS4 led to a loss of about 50% in the ability of RGS2 to reduce CCK-mediated inositol phosphate accumulation whereas insertion of this RGS2 sequence in RGS4 significantly increased the inhibitory effect of RGS4, chimeric RGS4/2 being almost as effective as wild-type RGS2. As with the wild-type RGS proteins, co-expression of chimeric RGS proteins did not modify CCK potency (Fig. 10), affinity (data not shown) or CCK2R expression levels.

Molecular Pharmacology Fast Forward. Published on December 8, 2008 as DOI: 10.1124/mol.108.051607
This article has not been copyedited and formatted. The final version may differ from this version.

DISCUSSION

G protein coupled receptors represent one of the most important families of signaling proteins with ubiquitous distribution throughout the animal and plant kingdom. The understanding of their functioning and their regulatory mechanisms represents a continuous challenge. In this study, we first demonstrated that CCK2R-mediated inositol phosphate production, known to be Gq-dependent, is more sensitive to RGS2 than to RGS4 and insensitive to RGS8. Moreover, we showed that the N-terminal region of RGS2 contains a region located between residues 54 and 79 that is required for RGS proteins activity on CCK2R signaling and for the formation of a complex with CCK2R. Surprisingly, we also found that the region of RGS2 between residues 54 and 79 modulates not only agonist-stimulated CCK2R-mediated signaling, but also agonist-independent CCK2R-mediated signaling (basal activity or constitutive activity of the receptor) a phenomenon never reported. These data are in line with those from other studies which reported the importance of the N-terminal region of RGS2 in regulation of GPCRs signaling. Indeed, deletion of this domain was shown to reduce the ability of RGS proteins to attenuate Gq-dependent signaling and eliminates receptor selectivity (Bernstein et al., 2004; Hague et al., 2005; Zeng et al., 1998). Moreover, N-terminus of RGS proteins was reported to play a role in the formation of a ternary complex made up of RGS/GPCR/scaffold protein or RGS/GPCR/G proteins independent of agonist stimulation (Bernstein et al., 2004; Hague et al., 2005; Wang et al., 2005). On the other hand, three amino acids (V9, Q10 and H11) located in the N-terminal region of RGS2 were found to be crucial for binding and inhibition of type V adenylate cyclase activity (Salim et al., 2003). Interestingly, between this adenylate cyclase binding region and the loop identified as been involved in CCK2R activity (this study), there is an amphipathic helix (residues 33 to 53) which was demonstrated to participate in the anchoring of RGS2 to the plasma membrane (Heximer et al., 2001). Our results that RGS2[54-211]

Molecular Pharmacology Fast Forward. Published on December 8, 2008 as DOI: 10.1124/mol.108.051607
This article has not been copyedited and formatted. The final version may differ from this version.

lacking the amphipathic helix still inhibited CCK2R mediated inositol phosphate production support previous findings that RGS2 membrane targeting is not essential for RGS2 activity.

The current study also provides a set of converging experimental results indicating that two amino acids located in the C-terminal region of the CCK2R, namely S434 and T439 are crucial for the ability of RGS2 to modulate CCK-induced inositol phosphate production but not the basal response. Interestingly, these two amino acids must be phosphorylated for functional recognition of RGS2 following agonist stimulation. Firstly, surface plasmon resonance experiments showed that a synthetic replicate of the C-terminal region of CCK2R which was phosphorylated on both S434 and T439 could bind directly with high affinity to recombinant RGS2 in the absence of any other protein. Secondly, immunoprecipitation of CCK2R following [^{32}P] labeling showed that S434 and T439 were indeed phosphorylated following CCK exposure. In addition, replacement of S434 in the CCK2R by a Glu residue, known to mimic phosphorylated Ser/Thr, restored RGS2 regulation of CCK2R-dependent activity. At last, molecular modeling provided structural support and likely physico-chemical explanations for the direct interaction between RGS2 and CCK2R: the interaction between the RGS2 loop and the CCK2R fragment, phosphorylated on both S434 and T439, is energetically favorable; pS434 forms an ionic interaction with K62 of RGS2 and pT439 interacts with both K63 and Q67 through ionic interaction and hydrogen bond, respectively (Fig. 9). Experimental results with the Q67A-RGS2 mutant and the RGS2/4 chimera displaying reduced ability to modulate CCK-induced inositol phosphate accumulation relative to intact RGS2, alongside those with the RGS4/2 chimera with equal efficiency to RGS2, not only confirm theoretical predictions, but also provide a molecular basis for a higher efficacy of RGS2 compared to RGS4. This is likely due to Q67 that is conserved in RGS2 among all species and is replaced by a valine in RGS4. The apparent discrepancy between results showing that Glu substitution of T439 did not restore RGS2 regulation of CCK2R-dependent

Molecular Pharmacology Fast Forward. Published on December 8, 2008 as DOI: 10.1124/mol.108.051607
This article has not been copyedited and formatted. The final version may differ from this version.

activity and results from surface plasmon resonance showing that phosphorylation of both T439 and S 434 is required for high affinity binding of the synthetic replicate of the CCK2R C-terminal region to recombinant RGS2 can be explained by examining the contact region between RGS2 and the CCK2R in the modeled complex. Indeed, due to its composition and planar shape, the carboxylate function of Glu gives less opportunity of interaction and lower energy bonds relative to the phosphate moiety of T439, which presents one uncharged and three negatively charged oxygens distributed around the phosphor atom (Fig. 7). Precedents exist showing an inability of Glu substitution to mimic phosphorylated Thr, as for example in the 78-kDa protein kinase Mekk1 (Siow et al., 1997).

Several studies have recently addressed the mechanism whereby Gαq-coupled receptors interact with preferred RGS with a high degree of specificity (Neitzel and Hepler, 2006). In fact, our current findings that a direct and functional interaction occurs between the RGS2 N- terminal and CCK2R C-terminal region, but not the third intracellular loop, must be compared with available data with muscarinic M1, α_1-, β_2-adrenergic and μ-, δ-opioid receptors (Bernstein et al., 2004; Wang et al., 2005). RGS2 was shown to be recruited to the plasma membrane by the Gs-coupled β_2-adrenergic receptor and to bind to the third intracellular loop of the β_2-adrenergic receptor (Roy et al., 2006). Hague et al. demonstrated that the N-terminus of RGS2 is required for association with α_{1A}-AR and selective inhibition of signaling, and that three residues located in the third intracellular loop of α_{1A}-AR are essential for that interaction (Hague et al., 2005). On the other hand, Wang *et al.* found that another adrenergic receptor, the α_{1B}-AR needs the scaffold protein spinophilin, which binds both the third intracellular loop of α_{1B}-AR and N-terminus of RGS2, to allow α_{1B}-AR.RGS2 association (Wang et al., 2005). In another study, RGS2, through its N-terminal moiety, was found to simultaneously bind to the M1 receptor third intracellular loop and activate Gq with its RGS domain (Bernstein et al., 2004). However, Bodenstein *et al.* were unable to provide

Molecular Pharmacology Fast Forward. Published on December 8, 2008 as DOI: 10.1124/mol.108.051607
This article has not been copyedited and formatted. The final version may differ from this version.

functional evidence for RGS2 specificity at M1 versus M3 receptors but showed that differential proteasomal regulation of RGS protein level could represent an alternative mechanism controlling RGS proteins activity (Bodenstein et al., 2007). It is also worthy to mention two studies performed on opioid receptors showing that morphine alters the selective association between μ-opioid receptors and specific RGS proteins (Garzon et al., 2005) and that RGS4 forms a stable complex with Gα, Gβγ and the C-terminal tail of both the μ- and the δ-opioid receptors but only following receptor activation (Georgoussi et al., 2006). These different data raise the possibility that recognition of RGS2 by GPCR, like that of Gα subunit of trimeric G proteins might occur through non predictable and differently located receptor sequences (Wess, 1997). Indeed, it is noteworthy that in the third intracellular loop of the mentioned receptors, no obvious consensus RGS proteins binding motifs could be identified. To explain the fact that N-terminal region of RGS2 interacts with and regulate effector proteins such as G-protein coupled receptor, adenylyl cyclase, tubulin, and the cation channel TRPV6, it has been proposed that that the N-terminal region of RGS2 comprises several short interaction motifs and/or can adopt distinct structures to bind various targets (Heximer and Blumer, 2007).

The fact that RGS2 regulation of activated CCK2R occurs through the phosphorylated C-terminus of CCK2R leads us to propose a role of RGS2 in CCK2R desensitization complementary to that of β-arrestin. Indeed, the current paradigm for GPCR regulation is that, in addition to G protein coupling, GPCR activation by agonists also initiates the process of receptor desensitization, an adaptive response used by cells to stop G protein signaling (Pierce et al., 2002; Reiter and Lefkowitz, 2006). In many cases, agonist-specific receptor desensitization involves the following general mechanism: after binding of an agonist, GPCR undergoes conformational changes that allow it to bind to kinases (GPCR Ser/Thr kinases or GRK), and thereby become phosphorylated in intracellular loops and the carboxyl terminus.

Phosphorylation of the receptor promotes the high affinity binding of arrestins to the receptor, which both physically interdicts further coupling of G protein and may act as a signal transducer (Reiter and Lefkowitz, 2006). The binding of RGS2 (that enhances GTP hydrolysis rate leading to G proteins uncoupling) to phosphorylated CCK2R could be an alternative/additional way of receptor desensitization to the steric hindrance of G protein coupling by β-arrestin. How this concept could be extended to other GPCRs remains to be studied. Moreover, the question of how RGS2, which is apparently associated to CCK2R in its basal state through a region different to the CCK2R C-terminal moiety, binds to the phosphorylated CCK2R C-terminal tail under agonist stimulation remains to be elucidated.

In conclusion this study provides a set of converging results indicating that RGS2 binds directly to CCK2R to modulate its activity. It also allows the identification of the interacting sequences involved both at the CCK2R and the RGS2 level in conditions of agonist stimulation.

Molecular Pharmacology Fast Forward. Published on December 8, 2008 as DOI: 10.1124/mol.108.051607
This article has not been copyedited and formatted. The final version may differ from this version.

ACKNOWLEDGMENTS

We sincerely thank “le Centre Informatique National de l’Enseignement Supérieur” (Montpellier, France) for software and hardware support.

Molecular Pharmacology Fast Forward. Published on December 8, 2008 as DOI: 10.1124/mol.108.051607
This article has not been copyedited and formatted. The final version may differ from this version.

REFERENCES

Bernstein LS, Ramineni S, Hague C, Cladman W, Chidiac P, Levey AI and Hepler JR (2004) RGS2 binds directly and selectively to the M1 muscarinic acetylcholine receptor third intracellular loop to modulate Gq/11alpha signaling. *JBiolChem* **279**(20):21248-21256.

Blom N, Gammeltoft S and Brunak S (1999) Sequence and structure-based prediction of eukaryotic protein phosphorylation sites. *JMolBiol* **294**(5):1351-1362.

Bodenstein J, Sunahara RK and Neubig RR (2007) N-terminal residues control proteasomal degradation of RGS2, RGS4, and RGS5 in human embryonic kidney 293 cells. *MolPharmacol* **71**(4):1040-1050.

Dufresne M, Seva C and Fourmy D (2006) Cholecystokinin and gastrin receptors. *Physiol Rev* **86**(3):805-847.

Foucaud M, Tikhonova IG, Langer I, Escrieut C, Dufresne M, Seva C, Maigret B and Fourmy D (2006) Partial agonism, neutral antagonism, and inverse agonism at the human wild-type and constitutively active cholecystokinin-2 receptors. *Mol Pharmacol* **69**(3):680-690.

Fourmy D, Lopez P, Poirot S, Jimenez J, Dufresne M, Moroder L, Powers SP and Vaysse N (1989) A new probe for affinity labelling pancreatic cholecystokinin receptor with minor modification of its structure. *EurJBiochem* **185**(2):397-403.

Garzon J, Rodriguez-Munoz M and Sanchez-Blazquez P (2005) Morphine alters the selective association between mu-opioid receptors and specific RGS proteins in mouse periaqueductal gray matter. *Neuropharmacology* **48**(6):853-868.

Georgoussi Z, Leontiadis L, Mazarakou G, Merkouris M, Hyde K and Hamm H (2006) Selective interactions between G protein subunits and RGS4 with the C-terminal domains of the mu- and delta-opioid receptors regulate opioid receptor signaling. *Cell Signal* **18**(6):771-782.

Hague C, Bernstein LS, Ramineni S, Chen Z, Minneman KP and Hepler JR (2005) Selective inhibition of alpha1A-adrenergic receptor signaling by RGS2 association with the receptor third intracellular loop. *JBiolChem* **280**(29):27289-27295.

Heximer SP and Blumer KJ (2007) RGS proteins: Swiss army knives in seven-transmembrane domain receptor signaling networks. *Sci STKE* **2007**(370):pe2.

Heximer SP, Knutsen RH, Sun X, Kaltenbronn KM, Rhee MH, Peng N, Oliveira-dos-Santos A, Penninger JM, Muslin AJ, Steinberg TH, Wyss JM, Mecham RP and Blumer KJ (2003) Hypertension and prolonged vasoconstrictor signaling in RGS2-deficient mice. *JClinInvest* **111**(4):445-452.

Heximer SP, Lim H, Bernard JL and Blumer KJ (2001) Mechanisms governing subcellular localization and function of human RGS2. *JBiolChem* **276**(17):14195-14203.

Hollinger S and Hepler JR (2002) Cellular regulation of RGS proteins: modulators and integrators of G protein signaling. *PharmacolRev* **54**(3):527-559.

Jones G, Willett P, Glen RC, Leach AR and Taylor R (1997) Development and validation of a genetic algorithm for flexible docking. *JMolBiol* **267**(3):727-748.

Kehrl JH and Sinnarajah S (2002) RGS2: a multifunctional regulator of G-protein signaling. *IntJBiochemCell Biol* **34**(5):432-438.

Luo X, Popov S, Bera AK, Wilkie TM and Muallem S (2001) RGS proteins provide biochemical control of agonist-evoked [Ca2+]i oscillations. *MolCell* **7**(3):651-660.

Marco E, Foucaud M, Langer I, Escrieut C, Tikhonova IG and Fourmy D (2007) Mechanism of activation of a G-protein coupled receptor, the human cholecystokinin-2 receptor. *JBiolChem*.

Moroder L, Wilschowitz L, Gemeiner M, Gohring W, Knof S, Scharf R, Thamm P, Gardner JD, Solomon TE and Wunsch E (1981) [Cholecystokinin-pancreozymin synthesis. Synthesis of [28-threonine,31-norleucine]- and [28-threonine,31-leucine]cholecystokinin-pancreozymin-(25-33)-nonapeptide]. *Hoppe SeylersZPhysiol Chem* **362**(7):929-942.

Neitzel KL and Hepler JR (2006) Cellular mechanisms that determine selective RGS protein regulation of G protein-coupled receptor signaling. *SeminCell DevBiol* **17**(3):383-389.

Neubig RR and Siderovski DP (2002) Regulators of G-protein signalling as new central nervous system drug targets. *NatRevDrug Discov* **1**(3):187-197.

Noble F, Wank SA, Crawley JN, Bradwejn J, Seroogy KB, Hamon M and Roques BP (1999) International Union of Pharmacology. XXI. Structure, distribution, and functions of cholecystokinin receptors. *Pharmacol Rev* **51**(4):745-781.

Oliveira-Dos-Santos AJ, Matsumoto G, Snow BE, Bai D, Houston FP, Whishaw IQ, Mariathasan S, Sasaki T, Wakeham A, Ohashi PS, Roder JC, Barnes CA, Siderovski DP and Penninger JM (2000) Regulation of T cell activation, anxiety, and male aggression by RGS2. *ProcNatlAcadSciUSA* **97**(22):12272-12277.

Pierce KL, Premont RT and Lefkowitz RJ (2002) Seven-transmembrane receptors. *NatRevMolCell Biol* **3**(9):639-650.

Reiter E and Lefkowitz RJ (2006) GRKs and beta-arrestins: roles in receptor silencing, trafficking and signaling. *Trends EndocrinolMetab* **17**(4):159-165.

Roy AA, Baragli A, Bernstein LS, Hepler JR, Hebert TE and Chidiac P (2006) RGS2 interacts with Gs and adenylyl cyclase in living cells. *Cell Signal* **18**(3):336-348.

Salim S, Sinnarajah S, Kehrl JH and Dessauer CW (2003) Identification of RGS2 and type V adenylyl cyclase interaction sites. *JBiolChem* **278**(18):15842-15849.

Siow YL, Kalmar GB, Sanghera JS, Tai G, Oh SS and Pelech SL (1997) Identification of two essential phosphorylated threonine residues in the catalytic domain of Mekk1. Indirect activation by Pak3 and protein kinase C. *JBiolChem* **272**(12):7586-7594.

Tikhonova IG, Boulegue C, Langer I and Fourmy D (2006) Modeled structure of the whole regulator G-protein signaling-2. *BiochemBiophysResCommun* **341**(3):715-720.

Van Der Spoel D, Lindahl E, Hess B, Groenhof G, Mark AE and Berendsen HJ (2005) GROMACS: Fast, flexible, and free. *JComputChem* **26**(16):1701-1718.

Wang Q, Liu M, Mullah B, Siderovski DP and Neubig RR (2002) Receptor-selective effects of endogenous RGS3 and RGS5 to regulate mitogen-activated protein kinase activation in rat vascular smooth muscle cells. *JBiolChem* **277**(28):24949-24958.

Wang X, Huang G, Luo X, Penninger JM and Muallem S (2004) Role of regulator of G protein signaling 2 (RGS2) in Ca(2+) oscillations and adaptation of Ca(2+) signaling to reduce excitability of RGS2-/- cells. *JBiolChem* **279**(40):41642-41649.

Wang X, Zeng W, Soyombo AA, Tang W, Ross EM, Barnes AP, Milgram SL, Penninger JM, Allen PB, Greengard P and Muallem S (2005) Spinophilin regulates Ca2+ signalling by binding the N-terminal domain of RGS2 and the third intracellular loop of G-protein-coupled receptors. *NatCell Biol* **7**(4):405-411.

Wess J (1997) G-protein-coupled receptors: molecular mechanisms involved in receptor activation and selectivity of G-protein recognition. *FASEB J* **11**(5):346-354.

Xu X, Zeng W, Popov S, Berman DM, Davignon I, Yu K, Yowe D, Offermanns S, Muallem S and Wilkie TM (1999) RGS proteins determine signaling specificity of Gq-coupled receptors. *JBiolChem* **274**(6):3549-3556.

Zeng W, Xu X, Popov S, Mukhopadhyay S, Chidiac P, Swistok J, Danho W, Yagaloff KA, Fisher SL, Ross EM, Muallem S and Wilkie TM (1998) The N-terminal domain of RGS4 confers receptor-selective inhibition of G protein signaling. *JBiolChem* **273**(52):34687-34690.

Molecular Pharmacology Fast Forward. Published on December 8, 2008 as DOI: 10.1124/mol.108.051607
This article has not been copyedited and formatted. The final version may differ from this version.

FOOTNOTES

IL is "Chargée de Recherches" from the "Fonds National de la Recherche Scientifique" (FNRS), Belgium. IL and IT received fellowships from “Fondation pour la Recherche Medicale”.

We sincerely thank “Association pour la Recherche contre le Cancer” for its financial support (ARC 3756).

Addresses for reprint request:

Daniel Fourmy, IFR 31, Institut Louis Bugnard, BP 84225, Unité INSERM U858 - I2MR

31432 TOULOUSE CEDEX 4 France, Tel: (33)5 61 32 30 57, Fax: (33)5 61 32 24 03

Email: fourmyd@toulouse.inserm.fr

Molecular Pharmacology Fast Forward. Published on December 8, 2008 as DOI: 10.1124/mol.108.051607
This article has not been copyedited and formatted. The final version may differ from this version.

LEGENDS TO FIGURES:

Figure 1: Effect of co-expressing CCK2R and RGS proteins on CCK2R-mediated inositol phosphate production.

(A) Basal inositol phosphate (IP) and (B) maximal IP production in response to 1 µM CCK9 evaluated in COS-7 cells co-transfected with CCK2R (0.5 µg) and increasing concentrations of RGS2, RGS4 and RGS8 (0.5-2 µg). If necessary, total DNA quantity was adjusted to 2.5 µg with empty vector. Results represent the means ± SEM of at least 3 independent experiments performed in duplicate. * $p<0.05$ and *** $p<0.001$ determined by Mann-Whitney test. In all conditions CCK potency was calculated from dose-effect curves (RGS2, EC_{50} = 0.53 ± 0.09 nM; RGS4, EC_{50} = 0.50 ± 0.05 nM; RGS8, EC_{50}0.58 ± 0.06 nM) and CCK2R expression levels evaluated by binding studies (RGS2, 88.6 ± 9.7% of control, n=10; RGS8, 102.9 ± 5.6% of control, n=3; RGS4, 74.3 ± 8.5% of control, n=4 $p<0.05$; control values, $Bmax_1$ = 1.2 ± 0.1 and $Bmax_2$ = 2.3 ± 0.2 pmole/10^6 cells).

(C) Western Blot analysis of RGS proteins expression levels. COS-7 cells co-expressing MYC-tagged CCK2R and HA-tagged RGS proteins were solubilized, resolved on 12% acrylamide-SDS gels, transferred to nitrocellulose membrane and blotted with anti-HA antibody (top panels). The membranes were then stripped and re-probed using a mouse anti-GAPDH antibody (bottom panels). Representative of 3 independent experiments.

Figure 2: Involvement of RGS2 N-terminus in CCK2R-mediated signaling.

(A) Schematic representation of the different RGS2 constructs tested.

(B) Basal inositol phosphate (IP) and (C) maximal IP production in response to 1 µM CCK9 determined in COS-7 cells co-transfected with CCK2R (0.5 µg) and increasing concentrations of RGS2, RGS2[28-211], RGS2[54-211] and RGS2[80-211] (0.5-2 µg). If necessary, total

Molecular Pharmacology Fast Forward. Published on December 8, 2008 as DOI: 10.1124/mol.108.051607
This article has not been copyedited and formatted. The final version may differ from this version.

DNA quantity was adjusted to 2.5 µg with empty vector. Results represent the means ± SEM of 3 independent experiments in duplicate. ** $p<0.01$ and *** $p<0.001$ determined by Mann-Whitney test. In all conditions CCK potency was calculated from dose-effect curves (RGS2, EC_{50} = 0.53 ± 0.09 nM, RGS2[28-211] EC_{50} = 0.60 ± 0.06 nM, RGS2[54-211] EC_{50} = 0.51 ± 0.07 nM, RGS2[80-211]EC_{50} = 0.47 ± 0.06 nM) and CCK2R expression levels evaluated by binding studies (RGS2[28-211], 86 ± 10% of control, n=3; RGS2[54-211], 92.1 ± 9.4% of control, n=3; RGS2[80-211], 95.3 ± 6.3% of control, n=3; ; control values, $Bmax_1$ = 1.2 ± 0.1 and $Bmax_2$ = 2.3 ± 0.2 pmole/10^6 cells).

(D) Western Blot analysis of RGS proteins expression levels. COS-7 cells co-expressing MYC-tagged CCK2R and wt or truncated HA-tagged RGS2 were solubilized, resolved on 12% acrylamide-SDS gels, transferred to nitrocellulose membranes and blotted with anti-HA antibody (top panels). The membranes were then stripped and re-probed using a mouse anti-GAPDH antibody (bottom panels). Representative of 3 independent experiments.

Figure 3: Immunoprecipitation and pull-down assay of CCK2R.

COS-7 cells were transfected or not with HA-tagged CCK2R and solubilized. Left: after immunoprecipitation with anti-HA antibody, proteins were blotted with anti-HA antibody. Right: COS-7 cell extracts were incubated with or without immobilized biotinylated peptide corresponding to the [54-79] sequence of RGS2 or biotinylated scramble peptide. Retained proteins were eluted and then blotted with anti-HA antibody.

Figure 4: Effect of co-expressing wild-type or truncated CCK2R and RGS2 on CCK9-induced inositol phosphate production.

(A) Amino acid sequence of the C-terminal tail of the CCK2R.

(B) Dose-effect curves of CCK9-induced inositol phosphate production of COS-7 cells transfected with 0.5 µg of wild-type (squares), CCK2[1-409] (circles), CCK2[1-429] (triangles) or CCK2[1-439] (lozenges) receptors in absence (closed symbols) or presence (open symbols) of 2 µg of RGS2. In the absence of RGS2 the total DNA quantity was adjusted to 2.5 µg with empty vector. Results represent the means ± SEM of a minimum 3 independent experiments in duplicate.

(C) Western Blot analysis of RGS2 expression levels. COS-7 cells expressing wt or truncated MYC-tagged CCK2R in the absence or presence of HA-tagged RGS2 were solubilized, resolved on 12% acrylamide-SDS gels, transferred to nitrocellulose membrane and blotted with anti-HA antibody (top panels). The membranes were then stripped and re-probed using a mouse anti-GAPDH antibody (bottom panels). Representative of 3 independent experiments.

Figure 5: Interaction of the N-terminus of RGS2 with CCK2R constructs.

COS-7 cells were transfected or not with wild-type or truncated HA-tagged CCK2R and solubilized. Left: after immunoprecipitation with anti-HA antibody, proteins were blotted with anti-HA antibody. Right: pull-down assay using immobilized biotinylated peptide corresponding to the sequence [54-79] of RGS2 followed by Western blot using anti-HA antibody of COS-7 cells expressing HA-tagged CCK2[1-409] (lane 1), CCK2[1-439] (lane 2) or wild-type (lane 3) CCK2R.

Figure 6: Effect of S434 and T439 mutation of CCK2R on the inhibitory effect of RGS2.

(A) Dose-effect curves of CCK9-induced inositol phosphate production of COS-7 cells transfected with 0.5 µg of wild-type or mutated CCK2R in the absence (closed symbols) or presence (open symbols) of increasing concentrations of RGS2 (0.5-2 µg). If necessary, total

Molecular Pharmacology Fast Forward. Published on December 8, 2008 as DOI: 10.1124/mol.108.051607
This article has not been copyedited and formatted. The final version may differ from this version.

DNA quantity was adjusted to 2.5 μg with empty vector. Results represent the means ± SEM of a minimum 3 independent experiments in duplicate.

(B) Western Blot analysis of RGS2 expression levels. COS-7 cells co-expressing wt or mutated MYC-tagged CCK2R and HA-tagged RGS2 were solubilized, resolved on 12% acrylamide-SDS gels, transferred to nitrocellulose membranes and blotted with anti-HA antibody (top panels). The membranes were then stripped and re-probed using a mouse anti-GAPDH antibody (bottom panels). Representative of 3 independent experiments.

Figure 7: CCK-induced phosphorylation of CCK2 receptor.

Receptor phosphorylation levels were evaluated after preincubation of COS-7 cells with inorganic [^{32}P] followed by CCK stimulation and receptor immunoprecipitation with anti-HA antibody. The labeled receptors were visualized by autoradiography following SDS page. (A) Dose-effect study after 5 min. CCK stimulation. (B) CCK2 and S434AT439A receptor phosphorylation levels following 5 min. stimulation with 100 nM CCK (upper panels). On the same cell preparation, relative receptor expression levels were evaluated by immunoprecipitation/Western Blot using anti-HA antibody (lower panel) for signal normalization of phosphorylation. The 2 graphs on the right represent the integration of the bands in arbitrary units. Representative of 3 independent experiments.

Figure 8: Surface plasmon resonance analysis of CCK2R binding to RGS2.

(A) Real-time interaction of doubly (pS434pT439) and mono-phosphorylated (pS434T439) C-terminal fragments of CCK2R to recombinant RGS2. (B) Dose-dependent binding of C-terminal doubly phosphorylated peptide (pS434pT439) to RGS2. Sensograms from the two experiments represent the differential response against non-phosphorylated C-terminal

Molecular Pharmacology Fast Forward. Published on December 8, 2008 as DOI: 10.1124/mol.108.051607
This article has not been copyedited and formatted. The final version may differ from this version.

fragments of CCK2R used in the reference channel. This figure is representative of three separate experiments.

Figure 9: Molecular model of [RGS2.CCK2R] interactions.

(A) Results from docking of the C-terminal phosphorylated region of CCK2R to a modeled RGS2 interacting loop followed by a 5 ns molecular dynamic simulation. (B) Zoom view of the interacting regions. Helices in RGS2 are represented as red tubes. RGS2 loop and CCK2R C-terminus are represented in green and blue ribbons, respectively. For clarity, only the carbon traces of side-chains and interacting groups are depicted. Sequence alignment of RGS2 and RGS4 in the interacting region.

Figure 10: Effect of RGS2 and RGS4 chimeric proteins on CCK-induced inositol phosphate production.

(A) Dose-effect curves of CCK9-induced inositol phosphate production of COS-7 cells transfected with 0.5 μg of CCK2R in the absence (closed symbols) or presence (open symbols) of increasing concentrations of wt or chimeric RGS (0.5-2 μg). If necessary, total DNA quantity was adjusted to 2.5 μg with empty vector. Results represent the means ± SEM of a minimum 3 independent experiments in duplicate. In all conditions CCK2R expression levels evaluated by binding studies (RGS2, 88.6 ± 9.7% of control, n=10; RGS2/4, 85.9 ± 8.6% of control, n=3; RGS4/2, 92.3 ± 7.5%; RGS4, 74.3 ± 8.5% of control, n=4 $p<0.05$).

(B) Western Blot analysis of RGS proteins expression levels. COS-7 cells co-expressing MYC-tagged CCK2R and wt or chimeric HA-tagged RGS were solubilized, resolved on 12% acrylamide-SDS gels, transferred to nitrocellulose membranes and blotted with anti-HA

Molecular Pharmacology Fast Forward. Published on December 8, 2008 as DOI: 10.1124/mol.108.051607
This article has not been copyedited and formatted. The final version may differ from this version.

antibody (top panels). The membranes were then stripped and re-probed using a mouse anti-GAPDH antibody (bottom panels). Representative of 3 independent experiments.

Table I: Summary of the effects of truncation of CCK2R on the affinity and biological activity of CCK either in the absence or presence of RGS2.

	Basal Ins-P	CCK9s-stimulated Ins-P		Binding parameters			
	(% CCK2R)	EC_{50} (nM)	Emax (% CCK2R)	Kd_1 (nM)	Kd_2 (nM)	$Bmax_1$ (pmol/10^6 cells)	$Bmax_2$ (pmol/10^6 cells)
CCK2R	100	0.53 ± 0.08	100	0.38 ± 0.04	3.0 ± 0.4	1.2 ± 0.1	2.3 ± 0.2
CCK2R + RGS2	58 ± 3	0.53 ± 0.09	52 ± 2	0.30 ± 0.04	3.2 ± 0.4	1.3 ± 0.1	2.2 ± 0.2
TR409	154 ± 7	0.16 ± 0.05	200 ± 8	0.45 ± 0.03	3.3 ± 0.4	1.3 ± 0.2	2.2 ± 0.1
TR409 + RGS2	63 ± 3	0.24 ± 0.05	182 ± 5	0.44 ± 0.06	2.3 ± 0.3	1.4 ± 0.2	1.9 ± 0.2
TR429	110 ± 4	0.12 ± 0.04	207 ± 8	0.42 ± 0.04	2.5 ± 0.3	1.2 ± 0.2	2.7 ± 0.4
TR429 + RGS2	64 ± 5	0.28 ± 0.08	204 ± 7	0.37 ± 0.05	2.4 ± 0.4	1.4 ± 0.2	2.4 ± 0.3
TR439	120 ± 7	0.22 ± 0.03	166 ± 3	0.45 ± 0.03	2.4 ± 0.3	1.1 ± 0.1	2.7 ± 0.4
TR439 + RGS2	68 ± 4	0.44 ± 0.05	117 ± 2	0.41 ± 0.03	2.3 ± 0.3	1.2 ± 0.1	2.3 ± 0.2

Pharmacological study was performed on COS-7 cells transfected with wild-type or truncated CCK2R (0.5 μg) in absence or in presence of 2 μg of RGS2. Ins-P production or binding parameters were determined as described in materials and methods section. Results represent the means ± SEM of at least 3 independent experiments performed in duplicate.

Table II: Summary of the effects of the mutation of CCK2R on the affinity and the biological activity of CCK either in the absence or presence of RGS2

	Basal Ins-P	CCK9s-stimulated Ins-P		Binding parameters			
	(% CCK2R)	EC50 (nM)	Emax (% CCK2R)	Kd_1 (nM)	Kd_2 (nM)	$Bmax_1$ (pmol/10^6 cells)	$Bmax_2$ (pmol/10^6 cells)
CCK2R	100	0.53 ± 0.08	100	0.38 ± 0.04	3.0 ± 0.4	1.2 ± 0.1	2.3 ± 0.2
CCK2R + RGS2	58 ± 3	0.53 ± 0.09	52 ± 2	0.30 ± 0.04	3.2 ± 0.4	1.3 ± 0.1	2.2 ± 0.2
S432A	103 ± 4	0.51 ± 0.05	98 ± 3	0.40 ± 0.03	3.3 ± 0.4	1.3 ± 0.2	2.2 ± 0.2
S432A + RGS2	56 ± 4	0.62 ± 0.05	58 ± 2	0.44 ± 0.06	2.7 ± 0.3	1.4 ± 0.2	2.0 ± 0.2
S434A	98 ± 5	0.44 ± 0.04	95 ± 3	0.37 ± 0.04	2.8 ± 0.3	1.3 ± 0.2	2.4 ± 0.3
S434A + RGS2	***55 ± 5***	***0.45 ± 0.05***	***72 ± 2***	***0.36 ± 0.05***	***2.6 ± 0.4***	***1.2 ± 0.2***	***2.3 ± 0.3***
S437A	96 ± 6	0.61 ± 0.08	94 ± 3	0.45 ± 0.03	2.7 ± 0.3	1.2 ± 0.1	2.5 ± 0.4
S437A + RGS2	60 ± 4	0.59 ± 0.03	59 ± 3	0.41 ± 0.04	2.9 ± 0.4	1.3 ± 0.2	2.2 ± 0.2
Y438A	102 ± 5	0.55 ± 0.08	100 ± 2	0.44 ± 0.04	2.7 ± 0.3	1.4 ± 0.2	2.3 ± 0.2
Y438A + RGS2	53 ± 3	0.51 ± 0.09	57 ± 4	0.39 ± 0.04	2.8 ± 0.3	1.3 ± 0.2	2.2 ± 0.3
T439A	104 ± 4	0.48 ± 0.03	99 ± 3	0.40 ± 0.05	2.7 ± 0.4	1.2 ± 0.2	2.3 ± 0.3
T439A + RGS2	***60 ± 5***	***0.45 ± 0.05***	***97 ± 4***	***0.45 ± 0.03***	***3.0 ± 0.3***	***1.1 ± 0.3***	***2.2 ± 0.4***
S432AS437A	97 ± 5	0.61 ± 0.05	96 ± 2	0.42 ± 0.03	2.9 ± 0.4	1.3 ± 0.1	2.2 ± 0.2
S432AS437A + RGS2	56 ± 3	0.65 ± 0.08	56 ± 3	0.40 ± 0.04	3.2 ± 0.4	1.2 ± 0.1	2.1 ± 0.2
S434AT439A	101 ± 3	0.43 ± 0.05	97 ± 4	0.36 ± 0.03	3.1 ± 0.4	1.3 ± 0.2	2.2 ± 0.2
S434AT439A + RGS2	***59 ± 5***	***0.47 ± 0.06***	***100 ± 4***	***0.37 ± 0.05***	***2.9 ± 0.3***	***1.4 ± 0.2***	***2.1 ± 0.2***
S434E	99 ± 6	0.54 ± 0.05	98 ± 2	0.39 ± 0.04	3.1 ± 0.4	1.3 ± 0.2	2.2 ± 0.2
S434E + RGS2	***66 ± 4***	***0.58 ± 0.07***	***56 ± 2***	***0.40 ± 0.04***	***3.0 ± 0.4***	***1.2 ± 0.2***	***2.1 ± 0.2***
T439E	102 ± 5	0.49 ± 0.06	96 ± 3	0.38 ± 0.04	2.9 ± 0.5	1.3 ± 0.2	2.2 ± 0.2
T439E + RGS2	***62 ± 4***	***0.64 ± 0.07***	***91 ± 4***	***0.35 ± 0.05***	***2.8 ± 0.3***	***1.2 ± 0.1***	***2.3 ± 0.2***

Pharmacological study was performed on COS-7 cells transfected with wild-type or truncated CCK2R (0.5 µg) in absence or in presence of 2 µg of RGS2. Ins-P production or binding parameters were determined as described in materials and methods section. Results represent the means ± SEM of at least 3 independent experiments performed in duplicate

Figure 1

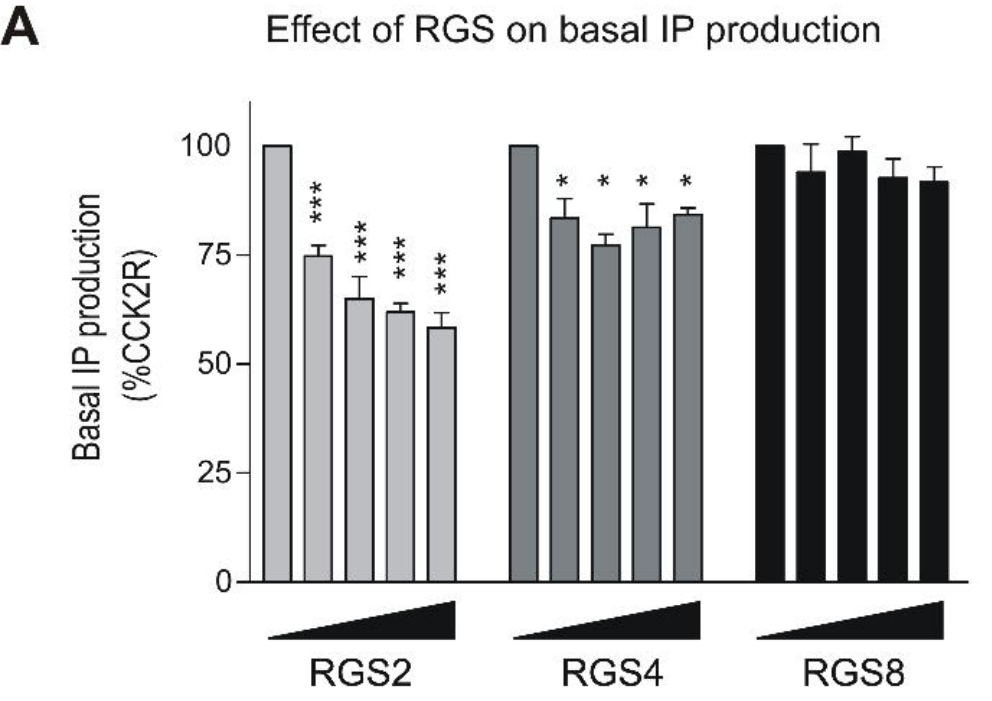
A
Effect of RGS on basal IP production
Basal IP production
(%CCK2R)
100
75
50
25
0
***
*
RGS2
RGS4
RGS8

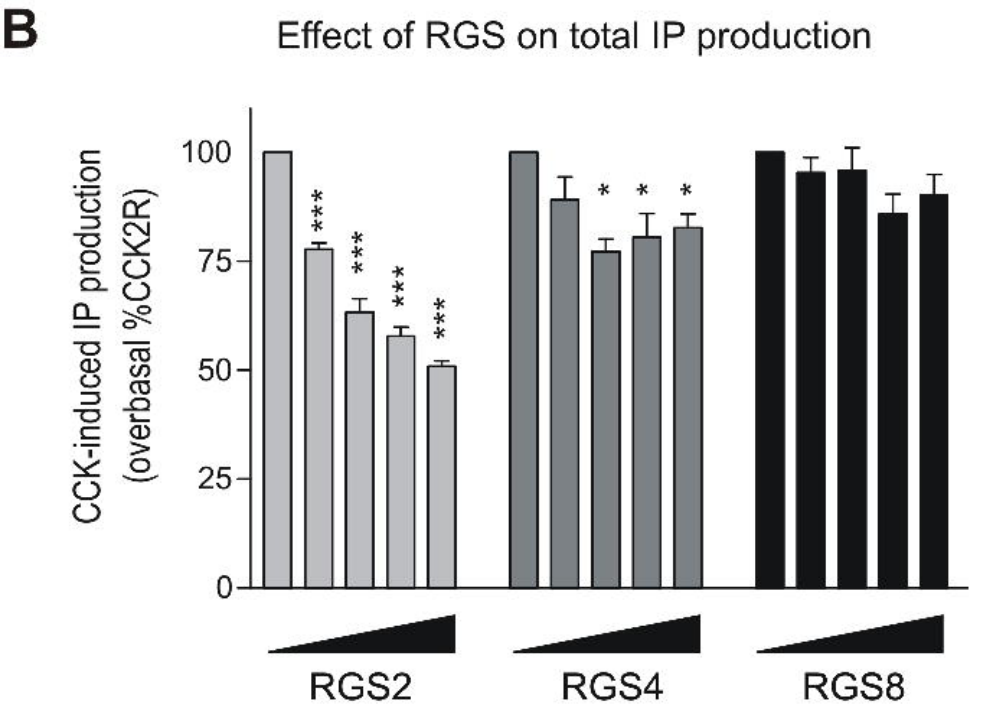
B
Effect of RGS on total IP production
CCK-induced IP production
(overbasal %CCK2R)
100
75
50
25
0
***
*
RGS2
RGS4
RGS8

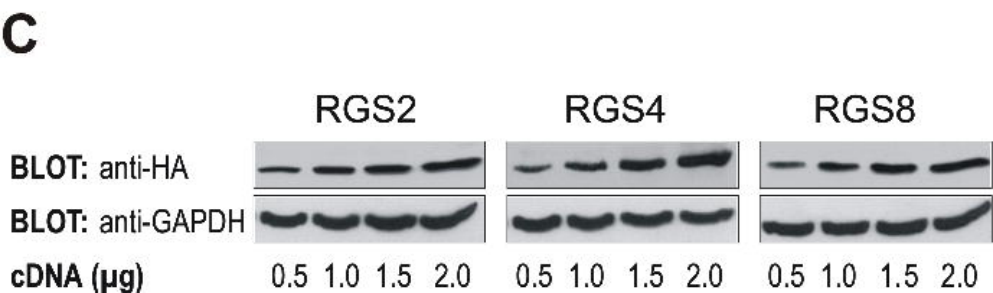
C
RGS2
RGS4
RGS8
BLOT: anti-HA
BLOT: anti-GAPDH
cDNA (µg)
0.5 1.0 1.5 2.0
0.5 1.0 1.5 2.0
0.5 1.0 1.5 2.0

Figure 2

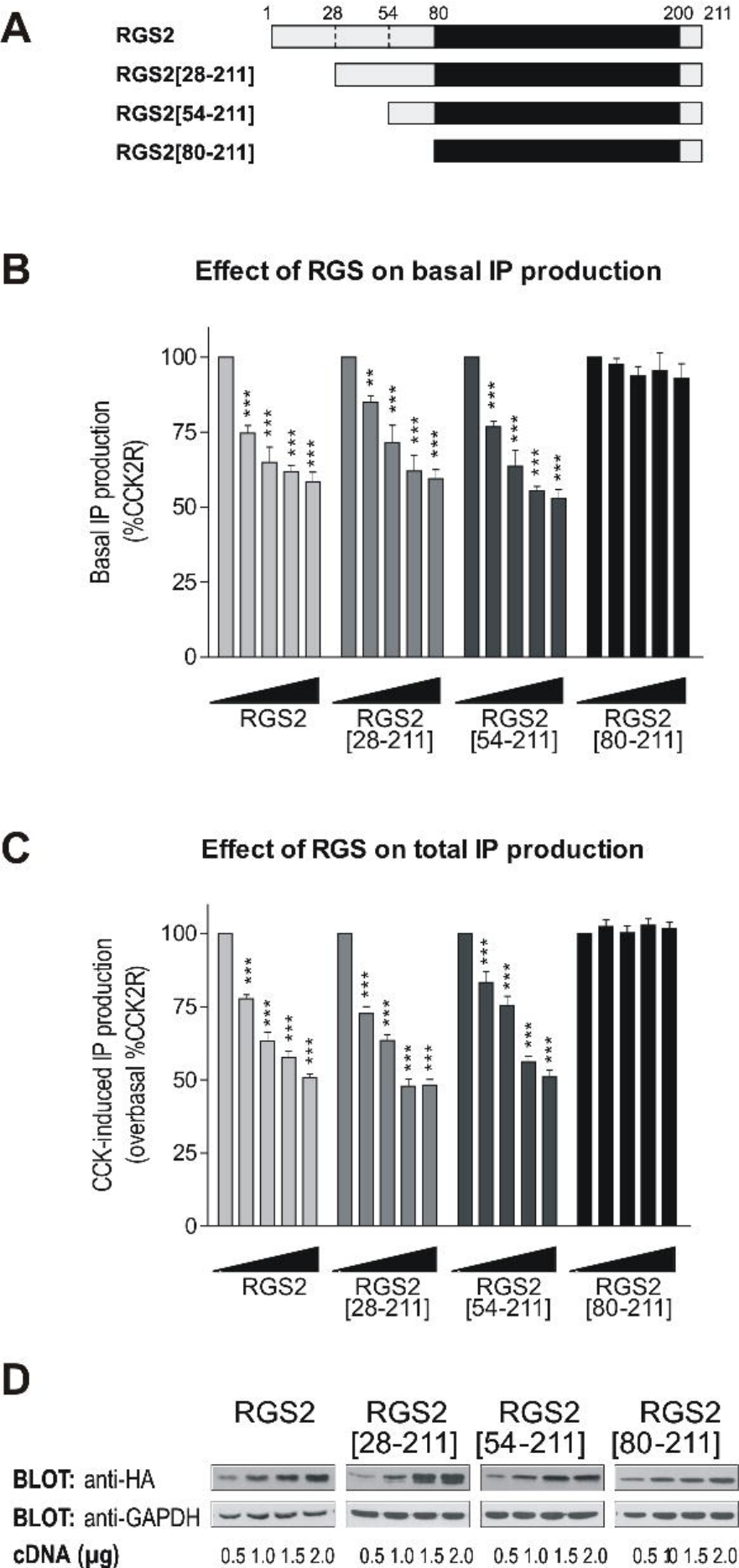
A
1
28
54
80
200
211
RGS2
RGS2[28-211]
RGS2[54-211]
RGS2[80-211]
B
Effect of RGS on basal IP production
Basal IP production (%CCK2R)
100
75
50
25
0
RGS2
RGS2 [28-211]
RGS2 [54-211]
RGS2 [80-211]
C
Effect of RGS on total IP production
CCK-induced IP production (overbasal %CCK2R)
100
75
50
25
0
RGS2
RGS2 [28-211]
RGS2 [54-211]
RGS2 [80-211]
D
RGS2
RGS2 [28-211]
RGS2 [54-211]
RGS2 [80-211]
BLOT: anti-HA
BLOT: anti-GAPDH
cDNA (µg)
0.5 1.0 1.5 2.0
0.5 1.0 1.5 2.0
0.5 1.0 1.5 2.0
0.5 1.0 1.5 2.0

Figure 3

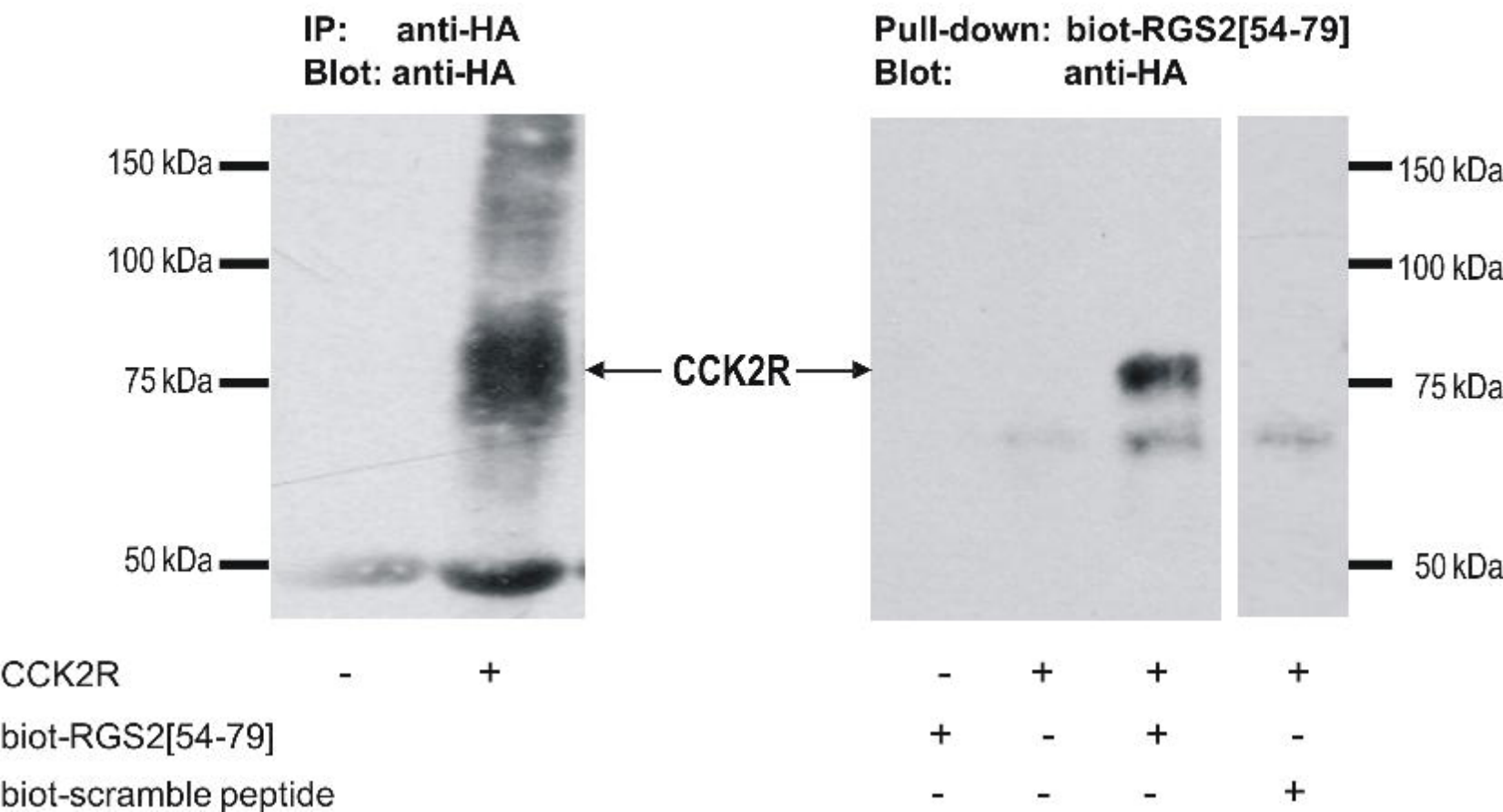
IP: anti-HA
Blot: anti-HA
Pull-down: biot-RGS2[54-79]
Blot: anti-HA
150 kDa
100 kDa
75 kDa
50 kDa
CCK2R
150 kDa
100 kDa
75 kDa
50 kDa
CCK2R - + - + + +
biot-RGS2[54-79] + - + -
biot-scramble peptide - - - +

Figure 4

A

CCK2R(CT) R^{396}FRQACLETCARC**C**^{409}PRPPRAR
PRALPDEDPPTP**S**^{429}IASLSRLSY**T**^{439}
TISTLGPG-COOH

B

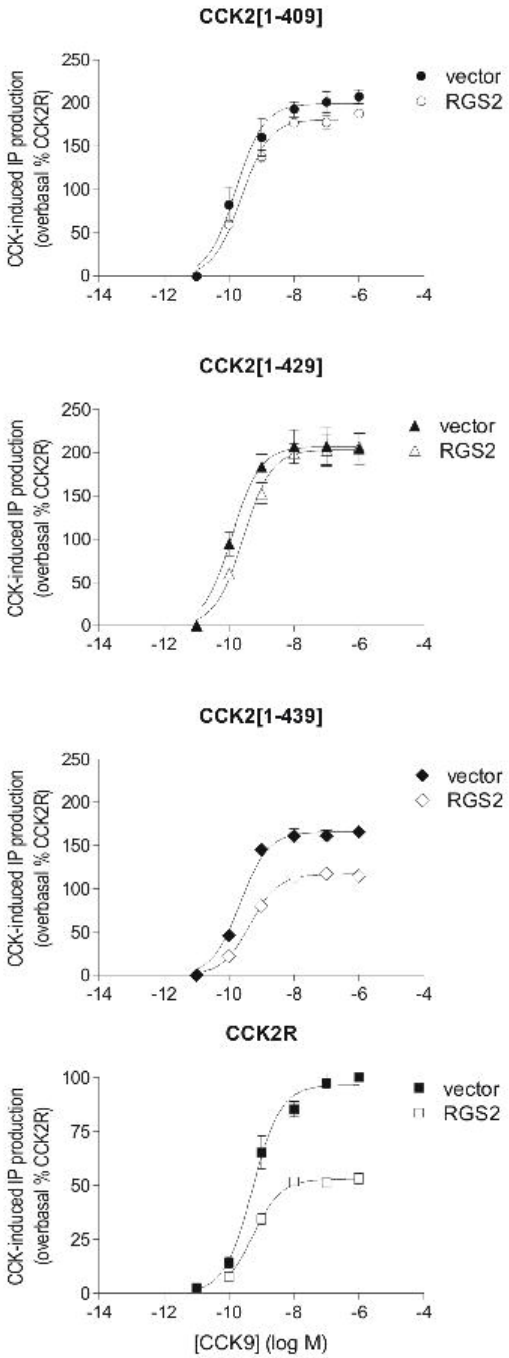

C

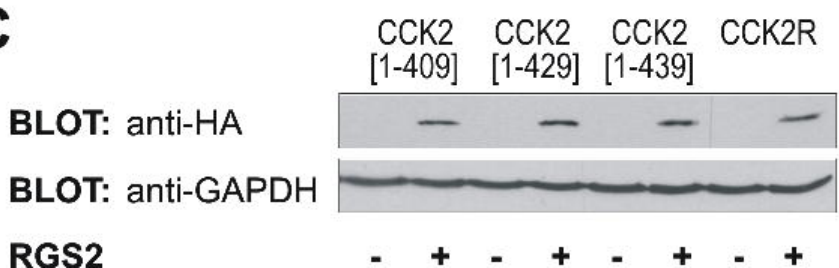

Figure 5

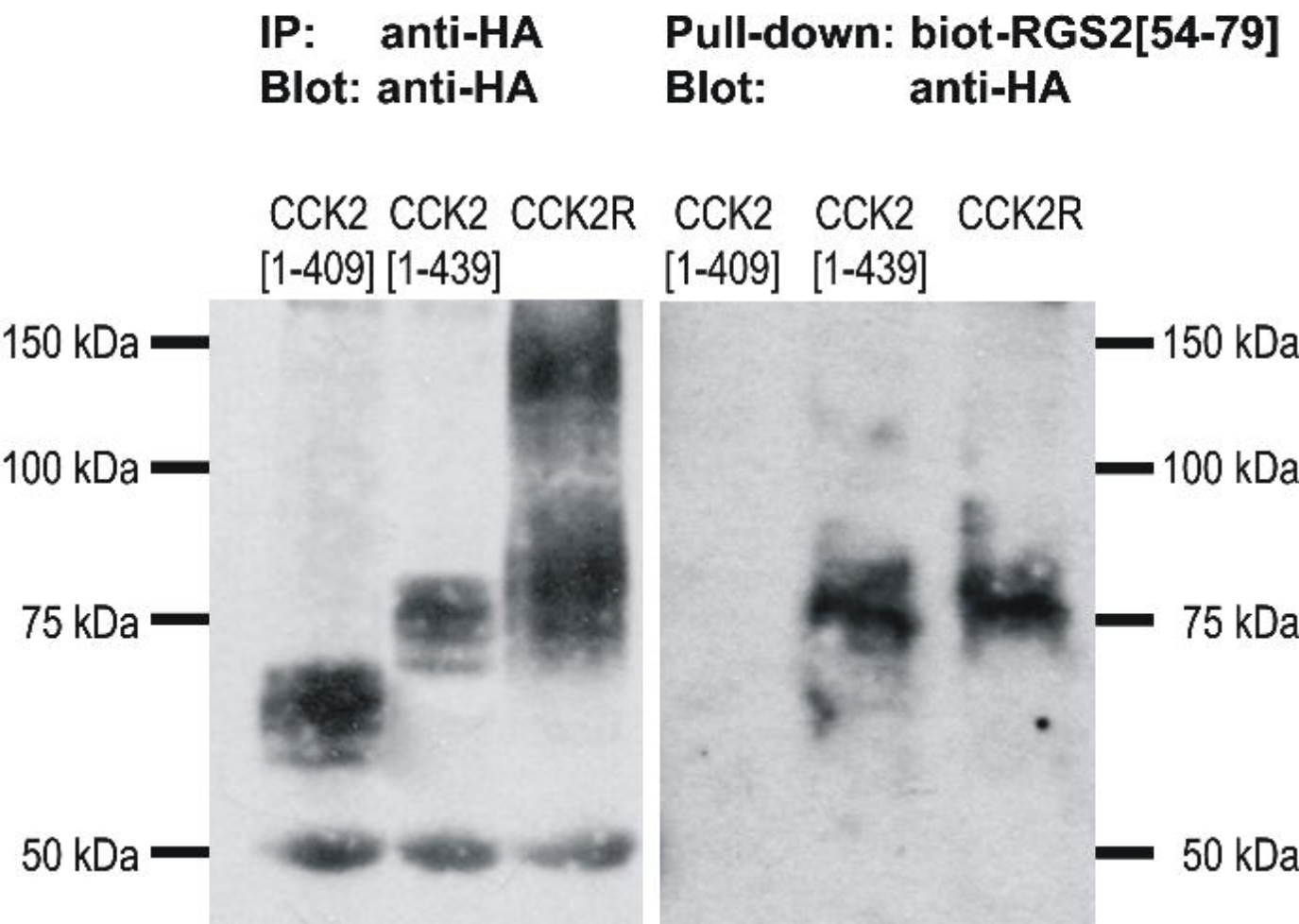
IP: anti-HA
Blot: anti-HA
Pull-down: biot-RGS2[54-79]
Blot: anti-HA
CCK2 [1-409]
CCK2 [1-439]
CCK2R
CCK2 [1-409]
CCK2 [1-439]
CCK2R
150 kDa
100 kDa
75 kDa
50 kDa
150 kDa
100 kDa
75 kDa
50 kDa

Figure 6

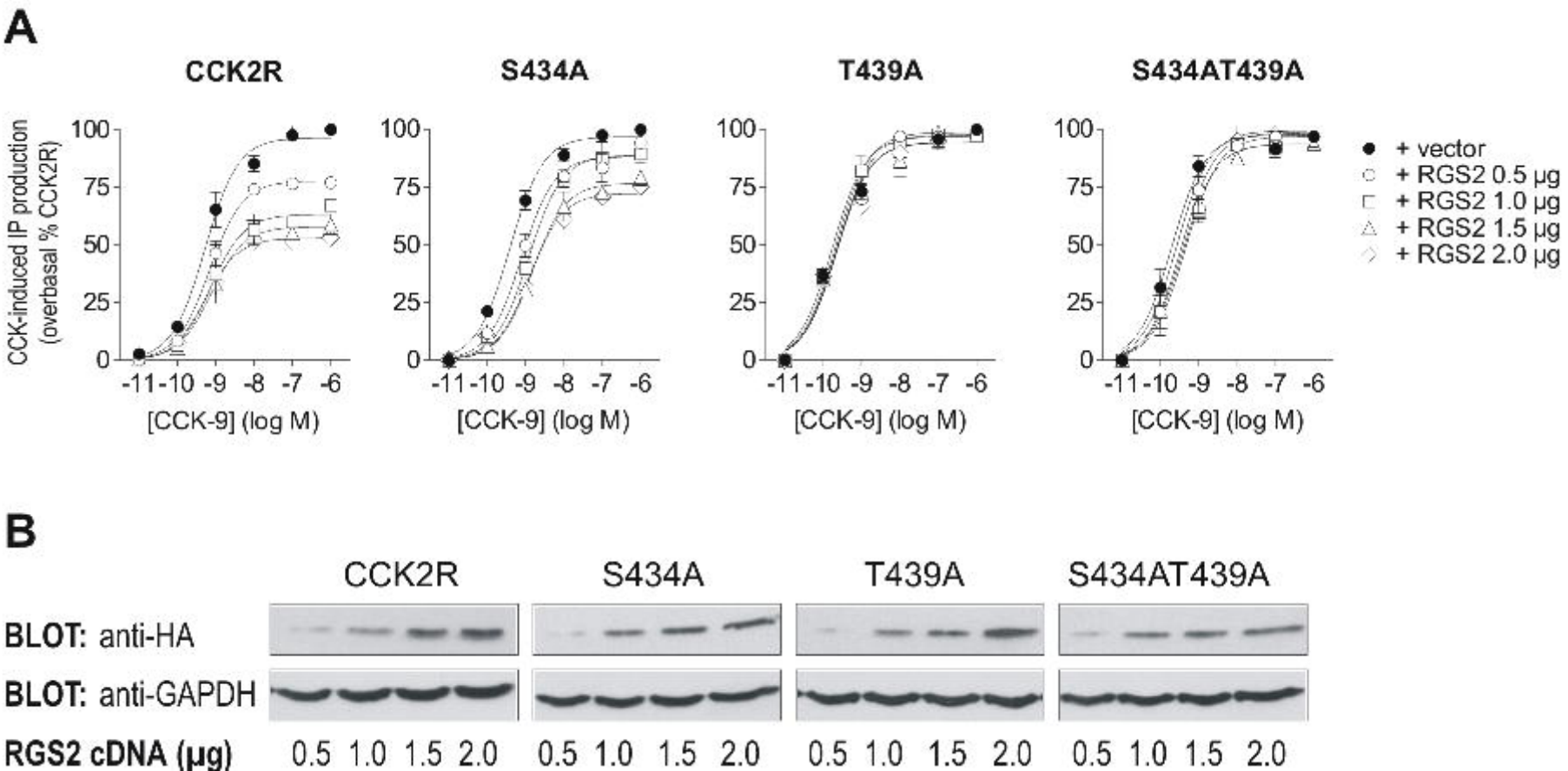
A
CCK2R
S434A
T439A
S434AT439A
CCK-induced IP production (overbasal % CCK2R)
100
75
50
25
0
-11 -10 -9 -8 -7 -6
[CCK-9] (log M)
+ vector
+ RGS2 0.5 µg
+ RGS2 1.0 µg
+ RGS2 1.5 µg
+ RGS2 2.0 µg
B
CCK2R
S434A
T439A
S434AT439A
BLOT: anti-HA
BLOT: anti-GAPDH
RGS2 cDNA (µg)
0.5 1.0 1.5 2.0

Figure 7

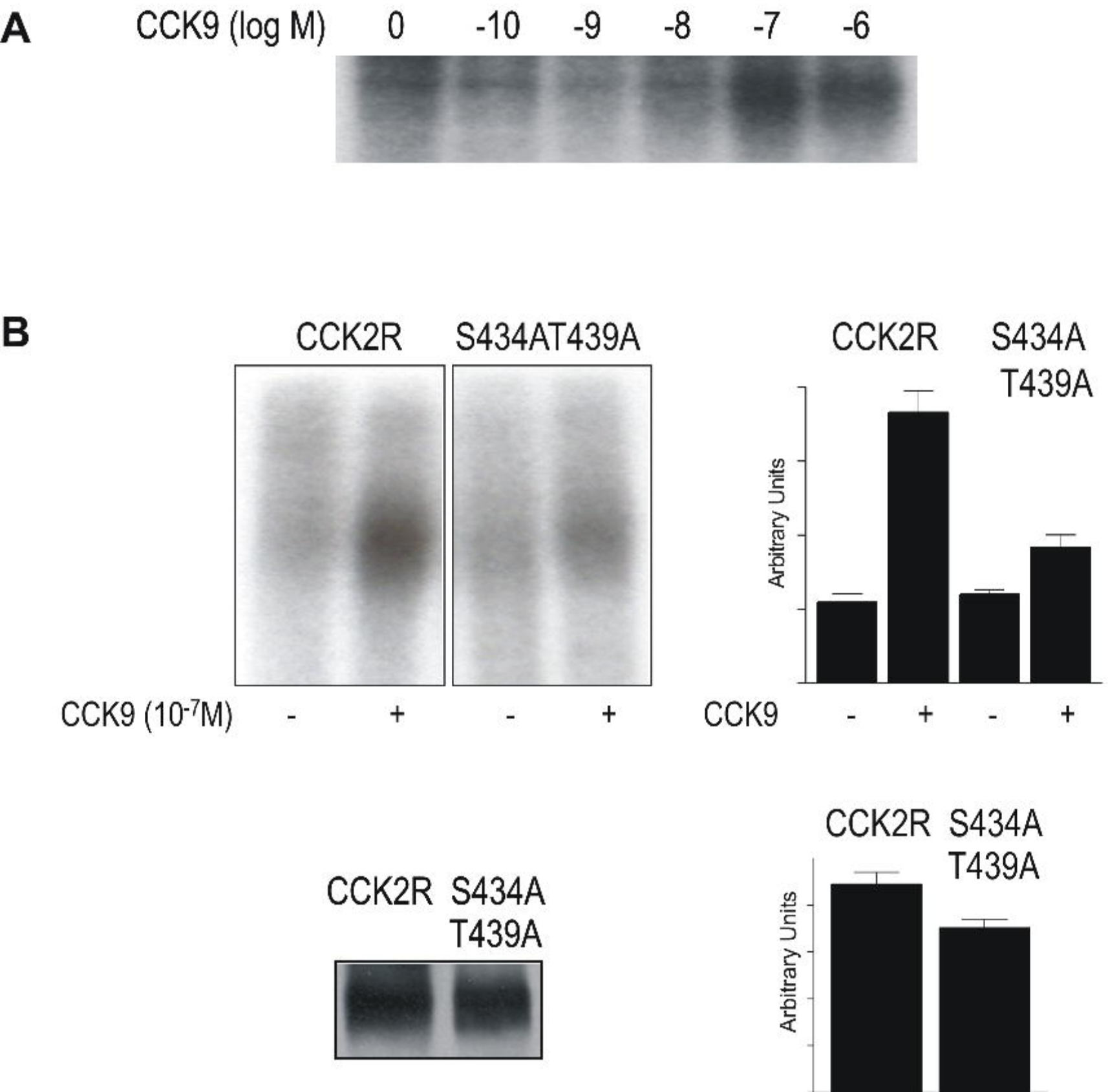
A
CCK9 (log M)
0
-10
-9
-8
-7
-6
B
CCK2R
S434AT439A
CCK9 (10-7M)
- + - +
CCK2R
S434A
T439A
Arbitrary Units
CCK9
- + - +
CCK2R S434A
T439A
CCK2R S434A
T439A
Arbitrary Units

Figure 8

A

CCK2R(429-445) *Biot-GGG*-SIASLSRLSYTTISTLG (reference)
pS434T439 *Biot-GGG*-SIASL**S(PO3)**RLSY**T**ISTLG
pS434pT439 *Biot-GGG*-SIASL***S(PO3)***RLSY***T(PO3)***TISTLG

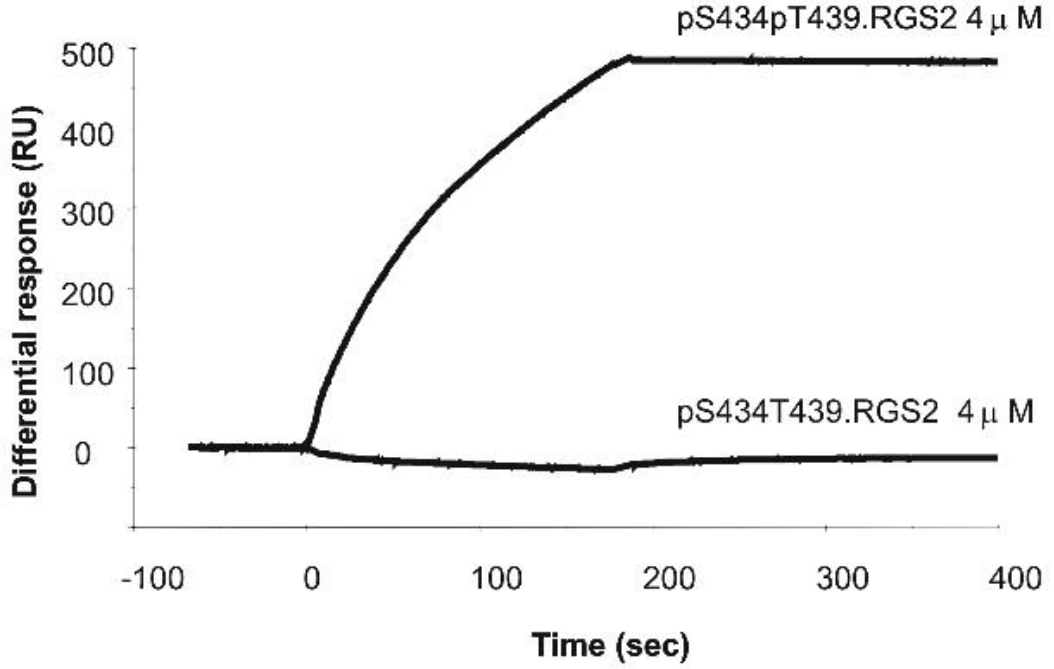

B

CCK2R(429-445) *Biot-GGG*-SIASLSRLSYTTISTLG (reference)
pS434pT439 *Biot-GGG*-SIASL***S(PO3)***RLSY***T(PO3)***TISTLG

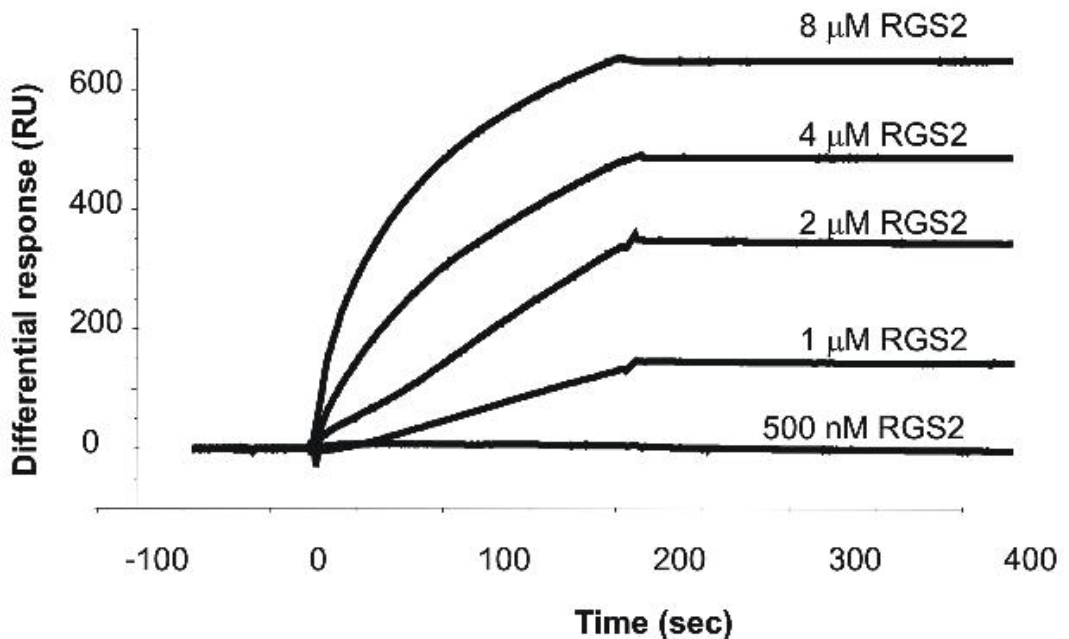

Figure 9

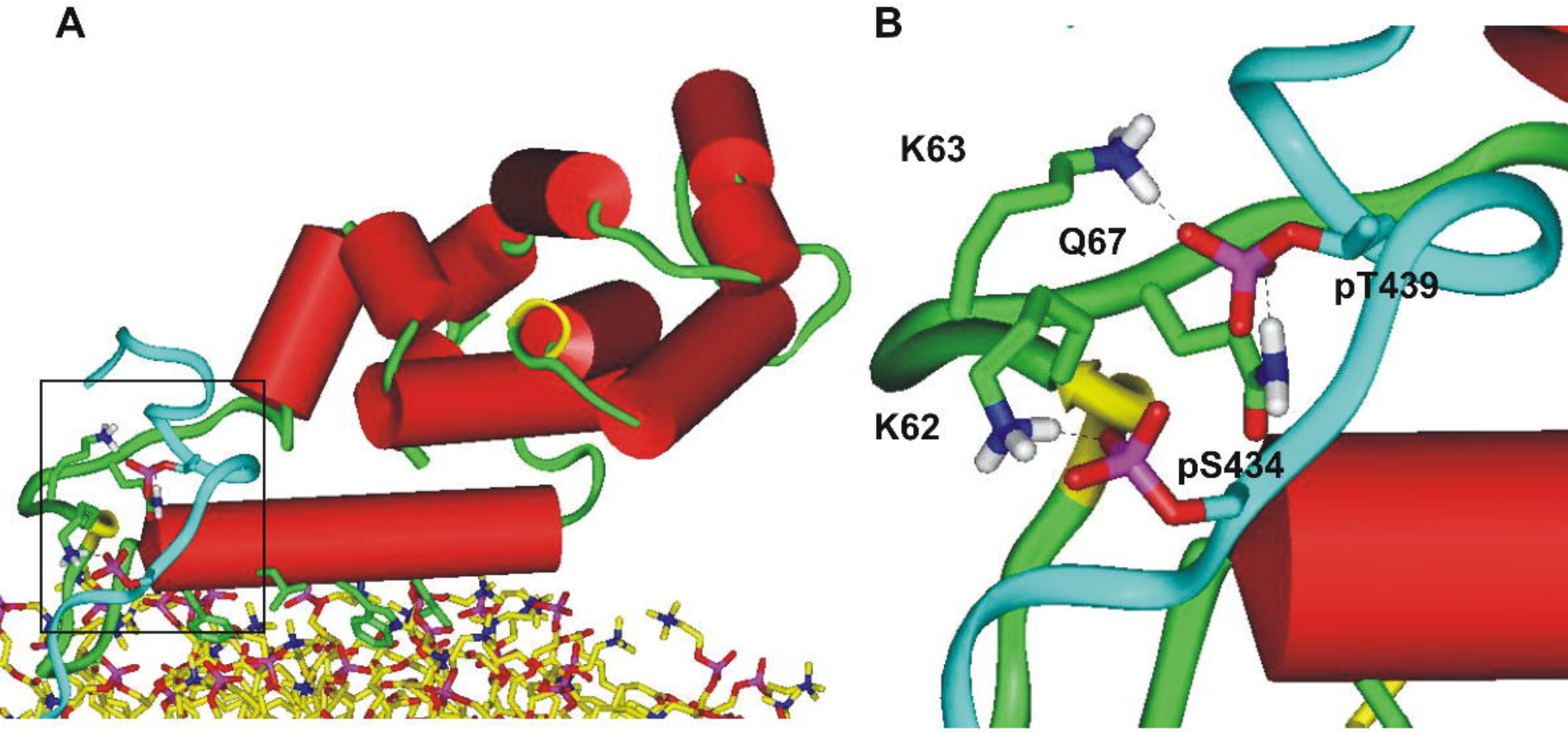

	62	67
RGS2 (mice)	SAPGKPKTG	KKSKQQTFIKPSP
RGS4 (rat)	SCEHSSSHS	KKDKVVTCQRVS

Figure 10

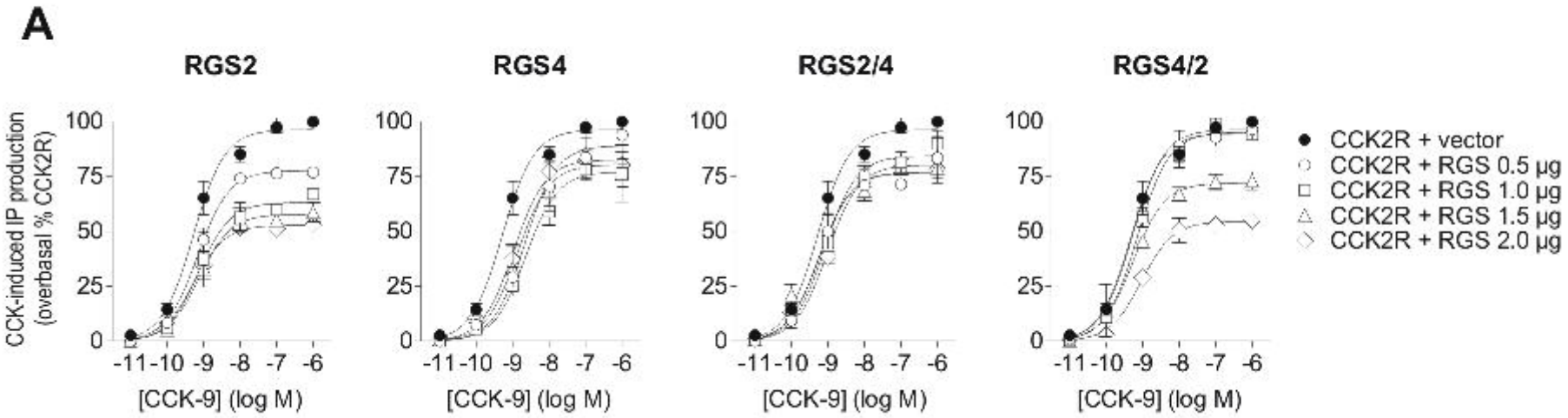
A
RGS2
RGS4
RGS2/4
RGS4/2
CCK-induced IP production (overbasal % CCK2R)
100
75
50
25
0
-11 -10 -9 -8 -7 -6
[CCK-9] (log M)
CCK2R + vector
CCK2R + RGS 0.5 µg
CCK2R + RGS 1.0 µg
CCK2R + RGS 1.5 µg
CCK2R + RGS 2.0 µg
B
RGS2
RGS4
RGS2/4
RGS4/2
BLOT: anti-HA
BLOT: anti-GAPDH
cDNA (µg)
0.5 1.0 1.5 2.0